NATIONAL ADVISORY COMMITTEE FOR AERONAUTICS

TECHNICAL NOTE 3225

AN EXPERIMENTAL STUDY OF THE LIFT AND PRESSURE DISTRIBUTION ON A DOUBLE-WEDGE PROFILE AT MACH NUMBERS NEAR SHOCK ATTACHMENT

By Walter G. Vincenti, Duane W. Dugan,
and E. Ray Phelps

Ames Aeronautical Laboratory
Moffett Field, Calif.

Washington
July 1954

lV

NATIONAL ADVISORY COMMITTEE FOR AERONAUTICS

TECHNICAL NOTE 3225

AN EXPERIMENTAL STUDY OF THE LIFT AND PRESSURE DISTRIBUTION ON A DOUBLE-WEDGE PROFILE AT MACH NUMBERS NEAR SHOCK ATTACHMENT

By Walter G. Vincenti, Duane W. Dugan,
and E. Ray Phelps

SUMMARY

An account is given of wind-tunnel measurements at low supersonic speeds of the pressure distribution on a doubly symmetrical double-wedge profile of approximately 8-percent thickness. The results cover the Mach number range from 1.166 to 1.377, which brackets the value (1.221) given by exact inviscid theory for attachment of the shock wave to the leading edge at zero angle of attack. Data are given for angles of attack from 0° to 5° at a Reynolds number of 0.54 million. The results are discussed in detail and compared with theoretical findings previously obtained on the basis of the transonic small-disturbance theory.

As predicted by the theory, the experimental results show a large increase in the initial lift-curve slope at Mach numbers near shock attachment. On the front wedge, where viscous effects are small, the numerical agreement between experiment and theory is good at the smaller angles of attack. This agreement tends to deteriorate, however, as the angle is increased. As might be expected from qualitative arguments regarding the limitations of the theory, this deterioration proceeds more rapidly the closer the Mach number is to the attachment value. As a result, the increase in lift-curve slope at Mach numbers near shock attachment disappears at the higher angles. On the rear wedge, where viscous effects are large, the data at small angles of attack show an unpredicted region of negative lift in the vicinity of the trailing edge.

In the case of the pressure drag due to angle of attack, agreement between theory and experiment is observed at small angles only when the Mach number is above the attachment value. At Mach numbers below this value, the drag rises less rapidly with angle of attack than is calculated on the basis of the theoretical pressure differences between the top and bottom of the airfoil. The measured drag and pressure distributions at zero angle of attack agree well with existing theoretical and experimental results throughout the Mach number range.

In support of recent findings by other investigators, the agreement between experiment and transonic theory is found to be greatly improved by the use of $(\gamma + 1)M_\infty^2$ in place of $(\gamma + 1)$ in the transonic similarity variables.

INTRODUCTION

This paper describes an experimental study of the pressure distribution over a double-wedge profile at free-stream Mach numbers near that for shock attachment. The work was motivated in part by the theoretical findings of references 1 and 2, which had indicated a rather unexpected increase in lift-curve slope at Mach numbers in this vicinity. Since calculations of other airfoil characteristics by means of the transonic theory had revealed no surprises, some experimental check of the findings appeared desirable. Moreover, as with all small-disturbance theories, a question could be raised concerning the range of angle of attack over which the results might be useful. This was particularly true in the present case, since the theory predicts only the initial slope of the lift curve, whereas the complete results at these Mach numbers might very well be nonlinear. The present study was made with these considerations in mind.

Because of simplifications afforded by a rectilinear profile, the properties of the transonic flow over wedges have attracted considerable attention. Besides the two investigations just cited, other studies have been made on the basis of the transonic small-disturbance theory by Guderley and Yoshihara, Cole, Trilling and Walker, and Vincenti and Wagoner (refs. 3 to 7). These studies taken together cover the complete range of subsonic, sonic, and supersonic flight speeds, and, except in the subsonic regime, include both the lifting and nonlifting case.[1] On the experimental side, studies of the transonic flow over wedges are numerous, though seldom as comprehensive as might be wished. (Refs. 9 through 27 are a chronological listing of the experimental reports known to the present authors.) These studies, particularly those of Liepmann and Bryson (refs. 15 and 17) and Griffith (ref. 19), provide a thorough description of the characteristics of single-wedge profiles at zero lift. The references regarding the lifting case are plentiful but less complete. Data in this regard are available for a wide range of subsonic speeds in references 9, 10, 11, 12, and 27; for sonic speed in reference 18; and for isolated supersonic speeds in references 9, 14, and 21. Because of their restricted range, the last three references provide little information on the variation of lift-curve slope with Mach number. The present study fills this gap by supplying detailed data on the lifting case over a range of supersonic speeds. Results of measurements at zero lift are also included. Wherever possible, comparison is made between the experimental and theoretical findings.

---

[1] A statement of the relation between the various theoretical studies and a description of the flow field pertinent to the present problem can be found in reference 2. Some question concerning the results of Trilling and Walker has been raised by Guderley in reference 8.

NOTATION

Primary Symbols

c	airfoil chord
c_l	section lift coefficient, $\frac{\text{lift per unit span}}{q_\infty c}$
c_d	section pressure-drag coefficient, $\frac{\text{pressure drag per unit span}}{q_\infty c}$
C_p	pressure coefficient, $\frac{p-p_\infty}{q_\infty}$
$\left(\frac{L}{D}\right)_{max}$	maximum lift-drag ratio
M	Mach number
p	static pressure
q	dynamic pressure
t	maximum thickness of airfoil
x	chordwise distance from leading edge, positive rearward
$\bar{x}$	chordwise distance from leading edge to center of lift, positive rearward
α	angle of attack
γ	ratio of specific heats (7/5 for air)
δ_{max}	maximum deflection angle attainable through an oblique shock wave
θ_w	half angle of wedge

Subscripts

∞	free-stream conditions
f	value for front wedge
r	value for rear wedge
b	value on bottom surface of airfoil

t value on top surface of airfoil

o value at zero angle of attack

APPARATUS

Wind Tunnel

The experimental results were obtained in the Ames 6- by 6-foot supersonic wind tunnel. This tunnel, which is of the continuous-operation closed-return type, is powered by two 25,000-horsepower electric motors driving a single 8-stage axial-flow compressor. The supersonic speed in the test section is obtained by means of an asymmetric adjustable nozzle of the type described by Allen in reference 28. This nozzle is made up of two asymmetrically curved nozzle blocks placed between parallel side walls. The expansion ratio of the nozzle and hence the supersonic Mach number in the test section can be varied continuously by sliding one of the curved blocks relative to the other. Variation of the Reynolds number in the test section is obtained by changing the pressure level in the tunnel. Condensation effects are rendered negligible by maintaining the air in the tunnel at a specific humidity of less than 0.0003 pound of water per pound of air.

Model and Supports

The model used in the investigation is shown in figures 1 and 2. The airfoil section was a doubly symmetrical double wedge with an included angle of 9° at the leading and trailing edges (corresponding to a thickness ratio t/c of 0.0787). This angle is identical to that of the thinnest section used by Bryson in his tests of wedges at zero angle of attack (ref. 17). To assure an acceptable profile, the model was made of hardened tool steel, surface ground to a leading-edge thickness of approximately 0.003 inch. A chord of 5 inches was selected to provide sufficient thickness for the installation of pressure orifices near the leading and trailing edges without at the same time making the wing so large as to cause tunnel-wall interference at low supersonic Mach numbers. The span was taken as 48 inches, this being the largest dimension that could be accommodated on the available surface grinder. Because of this limitation in size, the wing did not completely span the 6-foot test section, with the result that the flow conditions were not truly two-dimensional. It was thought, however, that the resulting aspect ratio of 9.6 was sufficiently large that chordwise pressure-distribution measurements at midspan would, at the intended airspeeds, give a close approximation to two-dimensional results. As will be seen, the experimental results appear to confirm this expectation.

Measurement of the pressure distribution at midspan was accomplished by means of 18 orifices located on one surface of the wing at the positions listed in figure 1. A complete set of orifices was placed in only one surface in order to simplify the design and construction of the model. As indicated in figure 1, however, two additional orifices were provided in the opposite surface at stations 20 and 40 percent of the chord from the leading edge. These orifices provided a check on the angle-of-attack settings as will be described later. All orifices led directly to stainless-steel tubes which emerged from the wing through a support sting at the rear. The orifice diameter was 0.018 inch.

The primary support for the wing was provided by the rearward sting, which was attached, in turn, to the regular angle-of-attack mechanism of the tunnel. As can be seen in figures 1 and 2, the sting was offset so that it joined the wing a small distance to one side of the midspan section. This distance was chosen such that at the supersonic Mach numbers anticipated locally on the rear of the airfoil, the pressure orifices at midspan would all lie outside the theoretical region of influence (viscous effects neglected) of the forwardmost part of the sting. Some idea of the actual effect of the sting was provided by some yet unpublished data on the spanwise variation of pressure on similarly constructed wings of lower aspect ratio. These data indicate that the effect is insignificant, except possibly on the high-pressure side of the rear wedge at the highest angles of attack.

To prevent flutter and excessive bending of the wing at high angles of attack, it was found necessary to support each tip of the model by means of two small-diameter, sweptback guy wires. The downstream end of each wire was fastened to a strut which was placed athwart the support sting at right angles to the extended chord plane of the wing. The strut was located well downstream of the trailing edge of the wing. (The wing, strut, and four guy wires can be visualized, roughly speaking, as forming the edges of a tetrahedron.) The pressures at the measuring orifices are unlikely to have been affected by the presence of the strut and guy wires.

Because of restrictions imposed by the low rigidity of the support sting, it was necessary to limit the total pressure of the air stream to a value of 4 pounds per square inch absolute. With the present airfoil, this provides a nearly constant Reynolds number of 0.54 million over the Mach number range of the tests.

Characteristics of Air Stream

In conformity with the usual practice in the 6- by 6-foot tunnel, the wing was mounted in the test section with its span parallel to the nozzle side walls. Surveys of the air stream in the asymmetric nozzle of the tunnel have shown that some variation of static pressure, Mach number, and stream angle exists in the test section in planes parallel

to the side walls.[2] Transverse flow from one such plane to another is, however, virtually nil. If the wing is placed parallel to the side walls, therefore, the variation in stream angle becomes a variation purely in angle of yaw relative to the wing. Experience has shown that such a variation has a negligible effect in tests like the present where only the longitudinal characteristics of the wing are of interest. The possible effects of the nonuniformities of pressure and Mach number in the plane of the wing, however, cannot be ignored.

To minimize these latter effects, considerable care was taken in positioning the wing in the tunnel. For this purpose, a detailed survey was made of the pressure field in the central vertical plane of the test section. The longitudinal position for the model was then chosen such that the nonuniformity of free-stream static pressure over the region to be occupied by the wing was as small as possible throughout the Mach number range of the test. At the position finally selected, the variation of free-stream static pressure over the plan form amounted in the worst case to approximately 3-1/2 percent of the mean dynamic pressure. This is equivalent to a variation in the dynamic pressure itself of about 1 percent and to a variation in Mach number of about 0.025. At the midspan location the maximum variation over the chord was 1-1/2 percent in static pressure, 1/2 percent in dynamic pressure, and 0.010 in Mach number. The variations were largest at the lower values of the test Mach number (M_∞ from 1.166 to 1.227) and decreased to about one half of the maximum values at the higher speeds (M_∞ from 1.253 to 1.377). In no case were the variations abrupt; that is, there were no shock waves or sudden expansions present. As will be explained later, the variation in static pressure was taken into account in the reduction of the test data.

METHODS

Test Procedure

The procedure followed in running the tests was to set the wind tunnel to a given Mach number and then pitch the model through the desired range of angles of attack. Since a complete set of orifices was present in only one surface, it was necessary, in order that complete data might be obtained, to test at both positive and negative angles. (The meaning of "positive" and "negative" with reference to the present tests will be explained later.) The angular setting was measured by means of a calibrated mechanical counter geared to the drive shaft of the angle-of-attack mechanism. To assure an accurate setting, care was taken to eliminate the effects of the backlash which is known to be present in the angle mechanism. This was done by approaching each setting from the "high" side -

[2]This situation is not inherent in an asymmetric nozzle, but is a result of the early and somewhat imperfect design employed in the present tunnel. Methods for designing improved nozzles are described in reference 29.

that is, from absolute values of the angle of attack higher than the desired setting. The same procedure was followed, of course, in the calibration of the mechanical counter prior to the test.

At each test condition, the pressures at the surface of the airfoil were measured by photographic recording from a back-lighted multiple-tube manometer. These pressures, like the static pressures in the test-section survey, were measured relative to the pressure at an orifice located in the side wall of the nozzle well upstream of the model. To obtain accurate data at small angles of attack and at the low total pressure used in the test (see section "Model and Supports"), a manometer fluid of low density was required. Dibutyl phthalate (specific gravity of 1.047 at the average room temperature of 75° F) was chosen as meeting this requirement and having at the same time relative freedom from the formation of troublesome bubbles at low pressures. Two photographs of the manometer were taken at each test condition, the first when the liquid columns were judged to have reached equilibrium and the other several minutes later. If any difference between the two photographs was apparent (which was rarely the case), the second was used in the reduction of the data. The total pressure in the settling chamber of the tunnel was measured by means of a mercury-filled micromanometer with sump vented to the atmosphere.

Data were obtained at nine test Mach numbers from 1.166 to 1.377 and at seventeen nominal angles of attack from -4° to $+4^\circ$. The test Mach number M_∞ is taken as the value of the measured, tunnel-empty Mach number averaged over the chord of the wing at midspan (see section "Characteristics of Air Stream"). To fix the sign of the angle of attack, the main set of 18 pressure orifices is thought of as lying in the "top" surface of the wing. Positive and negative angles are then defined in accord with the usual convention. The angular settings were made in $1/4^\circ$ increments near zero angle in order that the unusual phenomenon described in the introduction might not be overlooked in the event that it were confined to small angles. The limits of $\pm 4^\circ$ on the angle range were necessary in order to stay within the range provided by the available manometers with dibutyl phthalate as the working fluid.

Reduction of Data

To analyze the experimental results, the static pressures p measured at the orifices in the surface of the airfoil were first converted to coefficient form. This was done according to the standard formula

$$C_p = \frac{p-p_\infty}{q_\infty} \tag{1}$$

where p_∞ and q_∞ are reference values of static and dynamic pressure. In theoretical work, p_∞ and q_∞ are, of course, the static and dynamic pressures in the undisturbed flow at infinity upstream. In the present

experimental work, p_∞ was taken in each case as the static pressure existing in the empty tunnel at the same location as the orifice in question. This was done in order to incorporate at least an approximate correction for the small but not negligible variation of static pressure in the tunnel test section (see section "Characteristics of Air Stream"). The value of q_∞ in the experiments was calculated from the test Mach number and the measured total pressure in the settling chamber, isentropic flow being assumed between the settling chamber and the test section. This procedure, which amounts to using a spatially averaged value of q_∞, is permissible since the actual variation in dynamic pressure in the empty test section is very small. Values of the normal-force, chord-force, and pitching-moment coefficients were found by mechanical integration of faired plots of C_p versus x/c.[3] Since a complete set of orifices was present in only the top surface of the airfoil, it was necessary for this calculation to assume that the pressures existing on the bottom surface at a given positive angle of attack were identical to those measured on the top surface at the same nominal negative angle. The accuracy of this assumption will be discussed later. The lift and drag coefficients were calculated from the normal- and chord-force coefficients and the corrected value of the angle of attack (see below). The chordwise position of the center of lift was found, as usual, from the quotient of the pitching-moment and normal-force coefficients. It must be remembered, of course, that the results obtained in the foregoing fashion - that is, by integration of the pressure distribution - reflect only the contribution of the pressure forces. The influence of the skin friction is not included.

Unless otherwise stated, all angles of attack in the present work have been corrected for the elastic deflection of the support sting. The corrections were calculated from the measured values of the normal force and pitching moment on the basis of elastic constants previously determined by applying static loads at various chordwise locations on the model. The corrections serve to increase the angle of attack about 20 percent beyond the nominal setting. In the calculation of the correction it was necessary to assume that the normal force and pitching moment were constant across the span at values equal to those measured at midspan. Since there must actually be some loss of load at the tips, the resulting corrections are somewhat excessive. The previously mentioned data on the spanwise pressure distribution on wings of lower aspect ratio indicate that the consequent error in the final angle of attack is not over ±2 percent.

PRECISION OF RESULTS

The most likely source of serious error in the present work is in the assumption that the pressures on the bottom surface of the airfoil at a positive angular setting can be found accurately by measurements made on

[3]This omits the negligible contribution of the chord force to the pitching moment.

the top surface at the same negative setting. Because of this assumption, the accuracy of the final results depends in large part on the precision with which the positive angles of attack were duplicated by the corresponding negative angles. In view of the appreciable backlash in the angle mechanism and the considerable deflection of the support sting, there might be doubt as to the accuracy with which this could be accomplished.

To investigate this question, two secondary check orifices were provided, as previously described, in the bottom surface of the wing at 20 and 40 percent of the chord. Throughout the test no difference could be observed between the pressures measured at these check orifices at positive angles of attack and those measured at the corresponding primary orifices at negative angles. This validates the original assumption and implies that no significant error was involved in setting the angle of attack to equal values on either side of zero.

The situation at the zero angle itself, however, was less satisfactory. Here results obtained with a given orifice would sometimes differ depending on whether the zero setting was approached from the positive or negative direction. This indicates an inability to set the zero angle with precision, probably because the effect of the backlash in the angle mechanism cannot be eliminated near zero lift. It is estimated from the various pressure readings that the resulting uncertainty in the zero angle is never more than $\pm 1/20^{\circ}$.

As to other inaccuracies, it has been estimated from consideration of the various factors entering into the pressure measurements that the final values of C_p represent conditions existing in the tests accurately to within ± 0.005. The experimental values of M_∞ (as defined in the section "Test Procedure") are considered accurate to ± 0.004. Apart from the matters discussed in the preceding paragraphs, the angles of attack may be up to 2 percent too large as a result of the previously described uncertainty in correcting for the deflection of the support sting. Because of uncertainties involved in fairing and integrating the pressure distributions, the force and moment coefficients are probably less accurate than the pressure coefficients themselves, though quantitative limits are difficult to define. It is also difficult to judge how much imperfections in the test conditions - that is, nonuniformities in the wind stream - change the results from what would be obtained in a perfectly uniform flow. It is thought, however, that the method of computing C_p as previously described provides a reasonably accurate correction for the small stream irregularities existing in the present tests.

THEORETICAL CONSIDERATIONS

For the present airfoil and speed range, complete theoretical results are available on the basis of the transonic small-disturbance theory (refs. 1, 2, 3, and 7). These results are presented graphically in references 2 and 7 in terms of the generalized variables provided by the

transonic similarity rules. To apply the generalized curves of these references in the present investigation, the labels on the horizontal and vertical scales have been altered from those given in the original figures by replacing the quantity $(\gamma + 1)$ wherever it appears by the product $(\gamma + 1)M_\infty^2$. Thus, for example, the transonic similarity parameter ξ_∞ is taken equal to

$$\frac{M_\infty^2-1}{[(\gamma + 1)M_\infty^2(t/c)]^{2/3}} \text{ instead of } \frac{M_\infty^2-1}{[(\gamma + 1)(t/c)]^{2/3}}$$

and the generalized pressure coefficient $\tilde{C}_p$ to

$$\frac{[(\gamma + 1)M_\infty^2]^{1/3}}{(t/c)^{2/3}} C_p \text{ instead of } \frac{(\gamma + 1)^{1/3}}{(t/c)^{2/3}} C_p$$

This procedure is suggested by the derivation of the similarity rules given by Busemann in reference 30. It has been shown by Spreiter and Alksne (ref. 31), in several specific examples, to improve the accuracy of the small-disturbance theory as compared with both experiment and exact theory. Experience with the present data confirms the findings of these writers by showing consistently better agreement between theory and experiment when the altered form of the similarity variables is used.

Before taking up the results themselves, something should be said about the nature of the solution that the theory provides for the airfoil at angle of attack. As explained in detail in reference 2, this solution is obtained by regarding the effects of angle of attack as a small perturbation on a known solution at zero angle. Strictly speaking, this implies that the results are valid only in the limit of a vanishingly small angle of attack. As a practical matter, however, they may be expected to give a reasonable approximation to the truth for finite angles as long as the perturbation is truly small - that is, as long as it does not alter the fundamental character of the flow field. Consideration of the way in which the boundary-value problem is formulated in the hodograph plane indicates that this requirement is met provided that

$$\alpha \ll |\theta_w - \delta_{max}| \tag{2}$$

where θ_w is half of the total wedge angle at the leading edge and δ_{max} is the maximum flow deflection attainable through an oblique shock wave at a given free-stream Mach number. In practice, of course, this limitation should not be taken literally - there are many instances of an approximate theory having a wider range of applicability than the theory itself would suggest. The main importance of relation (2) is in showing that the angle range over which the theory applies may be expected to decrease as $\delta_{max} \to \theta_w$, or, equivalently, as the free-stream Mach number approaches the value for shock attachment at zero angle of attack.

The physical background for this behavior is of some interest. Consider first the case when the free-stream Mach number is greater than the

attachment value. (By "attachment value" we shall hereafter mean specifically the attachment value at zero angle of attack.) If, at such a Mach number, the angle of attack is increased from zero, an attitude will eventually be reached at which the bow wave, which was originally attached to the leading edge, will detach itself from the profile. Once this occurs, the angle of attack has obviously altered the basic character of the flow, and the theory would certainly not apply. This effect takes place at a smaller and smaller angle of attack the closer the free-stream Mach number is to the attachment value. Right at this Mach number, in fact, any finite angle is enough to bring about detachment of the wave.

At free-stream Mach numbers below the attachment value the situation is less obvious. Here one of the effects of angle of attack is to introduce, into the basic subsonic flow over the front of the airfoil (sketch (a)), a region of supersonic flow with sonic line beginning at the

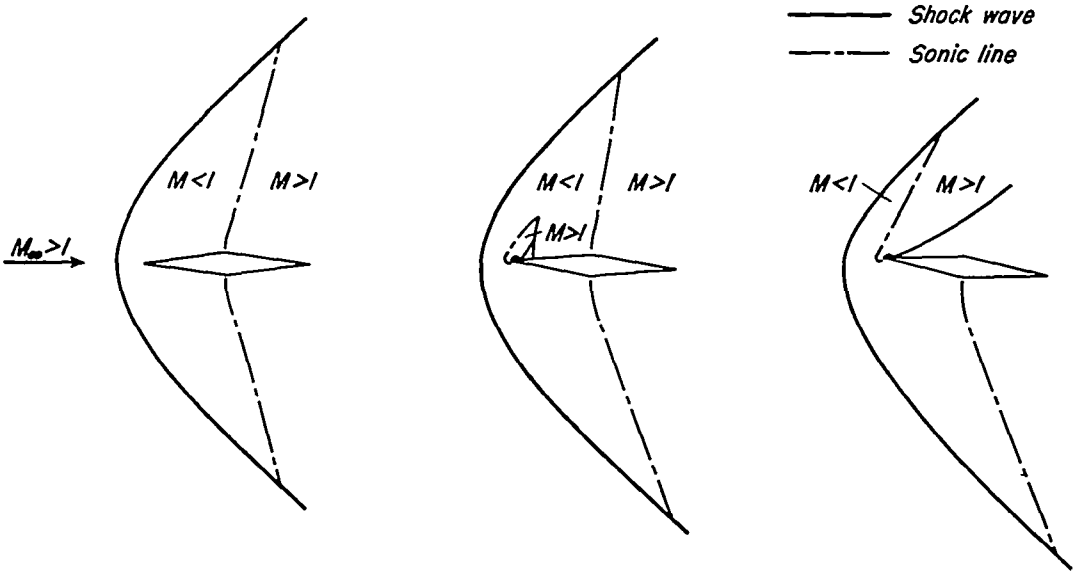

Zero α Small α Larger α

Sketch (a) Sketch (b) Sketch (c)

leading edge (sketch (b)). This supersonic region is properly neglected in the theory (see refs. 1 and 2) as having no influence on the rate of change of the airfoil characteristics at a vanishingly small angle of attack. At a small but finite angle of attack (sketch (b)), the region will not be entirely negligible, but its influence will be local in nature. By the time some larger angle is reached, however (sketch (c)), the region will have grown to the point of completely altering the character of the flow over the entire upper surface. Once this has occurred, the theory is again no longer applicable. As the Mach number increases toward the attachment value, the bow wave approaches closer and closer to the leading

edge, and, as before, the alteration of the fundamental character of the flow occurs at a smaller and smaller angle.

RESULTS AND DISCUSSION

The experimental results, together with the corresponding theoretical curves, are presented in figures 3 through 11. The Mach number range of the data is from 1.166 to 1.377, which brackets the theoretical attachment value of 1.221 given by exact inviscid theory. Since the purpose of the test was to answer certain fundamental questions rather than to provide design data, complete pressure-distribution results are not shown for each test Mach number and angle of attack. Sufficient examples are given, however, to illustrate all of the important phenomena. The values of the free-stream Mach number are specified throughout to three decimal places, not because they are considered accurate to that extent (see above), but to provide a more nearly correct relative spacing in plots having Mach number as the independent variable. For all of the data, the Reynolds number based on the chord of the model is approximately 0.54 million.

Characteristics at Zero Angle of Attack

The zero-lift characteristics of a single wedge (which is equivalent at the present speeds to the front half of the double wedge) have been investigated at considerable length by Liepmann and Bryson (refs. 15 and 17) and Griffith (ref. 19). The results for zero angle of attack from the present study are given here primarily as background for the later discussion of the lifting case. They also provide some possibly useful data on the zero-lift flow over the rear half of the double-wedge section.

Chordwise pressure distribution.- Figure 3 shows representative data for the chordwise distribution of pressure coefficient at zero angle of attack. Experimental and theoretical results are given for four values of the free-stream Mach number, two on each side of the theoretical attachment value of 1.221. Experimental points are shown for two conditions denoted by $+0^\circ$ and -0°. These were obtained by approaching the zero attitude from the positive and negative directions, respectively. The small differences between the two sets of data are a reflection primarily of the error in setting the zero angle as previously discussed (see section "PRECISION OF RESULTS"). Besides the theoretical curves from the transonic small-disturbance theory, parts (c) and (d) of figure 3 also include curves calculated by means of the standard linear and shock-expansion theories (see, e.g., refs. 32 and 33). These theories are valid, of course, only when the shock wave is attached to the leading edge and the flow is everywhere supersonic.

In general, the agreement between the experimental points and the curves of the transonic small-disturbance theory is remarkably good. Both experiment and theory show clearly the change from the nonuniform, transonic type of pressure distribution which exists on the front wedge when the bow wave is detached (figs. 3(a) and (b)) to the uniform, supersonic type of distribution which prevails in the presence of an attached wave (figs. 3(c) and (d)).

The quantitative differences which do exist between theory and experiment in figure 3 are due apparently to boundary-layer effects. On the front wedge at Mach numbers below the attachment value, for example, the measured pressures are slightly higher than the theoretical back to the 35-percent-chord station and then slightly lower aft of that point. The same behavior has been noted by Liepmann and Bryson (see fig. 9 of ref. 15). It was attributed by them to the displacement effect of the boundary layer, which acts like a thin parabolic body added to the basic wedge. Above the attachment Mach number, the experimental pressures are a bit higher than the theoretical over practically all of the front wedge. This is probably due again to the displacement effect of the boundary layer. The slight change from the previous case may stem from the fact that in purely supersonic flow the local pressure is fixed almost completely by the local slope of the displacing surface, while in the transonic case the pressures on the front wedge are a function of conditions at every point on the wedge. At all Mach numbers, the effect of the boundary layer at the ridge is to smooth out the theoretically discontinuous change in pressure by effectively rounding off the corner. On the rear wedge, the measured pressure shows a marked and progressive increase aft of the 75-percent-chord station. This is the result of a thickening of the boundary layer induced by the presence of the trailing-edge shock wave. Similar effects of boundary-layer thickening can be observed in certain of the pressure distributions given by Ferri in reference 34 (though most of Ferri's plots show an abrupt increase and subsequent constant pressure as is typical of a separated layer). All of the foregoing effects of the boundary layer would presumably be reduced by an increase in Reynolds number.

It is interesting to note from figures 3(c) and (d) that even when the bow wave is attached and the flow is everywhere supersonic, the transonic small-disturbance theory provides a distinct improvement over the linear theory in the calculation of the surface pressures. On the present airfoil, in fact, the transonic theory gives results only very slightly different from those provided by the more exact shock-expansion theory.

Pressure drag.- Data on the integrated pressure drag at zero angle of attack are plotted as a function of the free-stream Mach number in figure 4. Results are given separately for the front wedge, the rear wedge, and the complete profile.[4] In the case of the front wedge (fig. 4(a)), points are also included from Bryson's interferometric study of

[4]In each case, the aerodynamic coefficient is referred to the total chord of the complete airfoil.

flow over a single wedge of nose angle equal to that of the present profile (ref. 17). In each case, theoretical curves are included as given by the three theories previously discussed. The points marked "S" denote the values of M_∞ at which the transonic and shock-expansion theories predict an attached bow wave with uniform sonic flow over the front wedge.

The results of figure 4 reflect the qualities already noted in the detailed pressure distributions. For the front wedge, the measured drag coefficients are in good agreement with the predictions of the transonic and shock-expansion theories. The small differences between the present results and those of Bryson are within the limits of accuracy of the two tests (which were somewhat larger for Bryson's interferometric study than for the present direct pressure measurements). For the rear wedge, the measured drag coefficients are somewhat less than the theoretical, primarily because of the pressure rise associated with the shock-induced thickening of the boundary layer near the trailing edge. The results for the complete profile, of course, exhibit a similar behavior. Figure 4 also illustrates the obvious inadequacy of two-dimensional linear theory in the transonic range.[5]

The nature of the agreement between theory and experiment in the foregoing results implies that, at least at zero angle of attack, the finite span of the test model caused no serious deviation from two-dimensional results at the midspan measurement station.

Characteristics at Angle of Attack

To the best of the authors' knowledge, the most detailed measurements on a lifting wedge at Mach numbers near shock attachment are those given by Hilton in reference 21. These measurements were made on a wedge of low aspect ratio (3.3) and were confined to a single Mach number above the attachment value. They are thus unsuitable for checking the results of two-dimensional theory with regard to the variation of lift-curve slope with Mach number. The present data do allow such a check.

Chordwise load and pressure distribution.- Figure 5 shows the chordwise distribution of lift for the same four Mach numbers considered in figure 3. The ordinate here is the difference between the pressure

[5]Comparison of figure 4 with figure 8 of reference 7 also shows how replacing $(\gamma + 1)$ by $(\gamma + 1)M_\infty^2$ in the similarity variables (see section "THEORETICAL CONSIDERATIONS") helps to improve the numerical accuracy of the small-disturbance theory when applied to a specific airfoil. This is particularly apparent in the behavior of the curve of $(c_a)_o$ versus M_∞ at $M_\infty = 1$. The use of $(\gamma + 1)$ leads to a zero slope at this point (ref. 7), while the present method leads to a negative slope close to the exact theoretical value. A more detailed exposition of this point is given by Spreiter and Alksne in reference 31 (p. 59).

coefficients on the bottom and top surfaces divided by the angle of attack α. (As explained in the section "Reduction of Data," the experimental values for the bottom surface were actually obtained on the top surface at negative α.) The presentation of experimental results is limited to three representative angles of attack, two near zero and one near the upper end of the angle range. The angular settings are designated as approximate since they were not precisely the same for all Mach numbers, owing to differences in the deflection of the support sting. To minimize confusion, the experimental results are presented here as faired curves instead of individual data points. The experimental scatter was not serious, however, even at the rather small angle of 0.3°. The results of the transonic theory appear in each of the present plots as a single curve derived, as previously explained, on the assumption of a vanishingly small angle of attack. As before, results from linear theory are also shown for those Mach numbers (figs. 5(c) and (d)) at which the bow wave is attached to the airfoil at zero angle of attack.

For the front half of the airfoil, the agreement between experiment and transonic theory is - all things considered - remarkably good at the lower angles of attack. For $\alpha > 1.2^\circ$, however, the agreement tends to deteriorate with increasing angle. In confirmation of the earlier discussion, this deterioration proceeds more rapidly the closer the free-stream Mach number is to the attachment value. This is especially apparent above the attachment Mach number, as can be seen by comparing the effects of angle of attack in figures 5(c) and (d). The former case, in particular, reflects clearly the change from an attached to a detached shock as the angle of attack is increased. (The same phenomenon is apparent in the results of Hilton (ref. 21).) The interrelated effects of free-stream condition and angle of attack are also visible at Mach numbers below the attachment value (figs. 5(a) and (b)), though less consistently than before.

As at zero angle of attack, the results for the front wedge display secondary effects of the boundary layer. This is particularly true in the vicinity of the midchord point in figures 5(a) and (b), where theory predicts zero lift as a result of the transonic properties of the sharp ridge (see p. 29 of ref. 2 for details). As might be expected, the effective rounding of the ridge by the boundary layer prevents the experimental lift from falling all the way to zero.

On the rear half of the airfoil, viscous effects are of critical importance. This is made evident in figure 5 by the relatively large, unpredicted negative lift observed aft of the 75-percent-chord station at the smallest angle of attack. This effect is probably due to a change in the shock-induced thickening of the boundary layer relative to that which occurs at zero lift. The introduction of an angle of attack, by reducing the strength of the trailing-edge shock on the lower surface and increasing it on the upper surface, serves apparently to decrease the thickening in the one case and increase it in the other. As a consequence, the lift near the trailing edge is reduced below what one would expect in the

absence of a boundary layer. At very small angles of attack this effect evidently predominates, and a locally negative lift results. Precisely the same phenomenon is apparent in one of the experimental pressure distributions given by Ferri (see fig. 12 of ref. 34).[6] At larger angles of attack the effects of the boundary-layer thickening remain, but their influence is relatively less important. As a result, the agreement between theory and experiment on the rear half of the airfoil tends to improve with increasing angle. As at zero angle of attack, these viscous effects would probably be reduced by an increase in Reynolds number.

It is again interesting to note in figures 5(c) and (d) that even for Mach numbers somewhat above the attachment value, the transonic theory still provides a significant improvement over the linear approximation.

To illustrate the agreement between theory and experiment for the complete pressure distributions at angle of attack, the values of C_p itself are plotted in figure 6 for the two Mach numbers corresponding to figures 5(a) and (c). Here the experimental data are labeled according to the way in which the measurements were actually made - that is, on the top surface of the airfoil at positive and negative angles of attack. The theoretical curves are calculated by combining the results of references 2 and 7 on the assumption that over the entire angle range, the value of $dC_p/d\alpha$ is constant at the value computed for $\alpha \geq 0$.

Figure 6(a) illustrates the fact that at Mach numbers below the attachment value, the transonic theory predicts the pressure difference across the front wedge at the higher angles of attack more accurately than it does the individual pressures. Aside from this, figure 6 serves mainly to reemphasize the points already noted in connection with figure 5. Figure 6(b), in particular, shows again the effect of going from an attached to a detached wave as the angle of attack is increased.

Lift.- The integrated values of the lift coefficient are shown as a function of angle of attack in figure 7 for all the test Mach numbers. Experimental points are given for the front wedge as well as for the complete profile. The theoretical results for $\alpha \geq 0$ are shown by straight lines terminated (quite arbitrarily) at $\alpha = 3\text{-}1/2^\circ$. No theoretical values are given for $M_\infty = 1.227$ since this Mach number falls within the gap for which no results were calculated in reference 2.[7]

[6]An analogous phenomenon is to be found in the so-called "bevel effect" sometimes used as a means of balancing control surfaces at low subsonic speeds (ref. 35), though in this latter case the thickening (or separation) does not involve the presence of a shock wave.

[7]In figure 5 of reference 2, the ordinates shown at $\xi_\infty = 1.058$ are in error because of a mistake in the integration of the theoretical lift distribution for the front wedge. The correct values of the generalized lift-curve slope at this value of ξ_∞ are as follows: for the front wedge, 3.90; for the complete profile, 4.58. The results for the rear wedge are correct as originally plotted. The theoretical curves of the present figures 7 and 8 are based on the corrected values.

The results of figure 7 are such as one might expect in view of the foregoing discussion of the lift distribution. At all Mach numbers, theory and experiment agree reasonably well at the lower angles of attack ($\alpha < 1\text{-}1/4^\circ$). The agreement for the complete profile is poorer than for the front wedge because of the viscous effects on the rear half of the airfoil. This is especially true at the lowest angle of attack ($\alpha \cong 0.3^\circ$). At the two highest Mach numbers, the experimental data is nearly linear out to $4\text{-}1/2^\circ$, with the result that theory and experiment continue to agree over the entire angle range. The same is true to a lesser degree at the lowest Mach number. At the intermediate Mach numbers, however, the rate of increase of lift falls off with angle of attack, with the result that theory and experiment progressively diverge. As previously noted, this behavior is most pronounced at Mach numbers near the attachment value. It is apparent from figure 7 that the nonlinearity in the measured lift is traceable primarily to the front wedge, where the viscous effects are small. This implies that the nonlinearity and the resulting divergence of theory and experiment are indeed due to basic flow changes of the type discussed earlier in the report (see section "THEORETICAL CONSIDERATIONS").

The foregoing results are summarized in figure 8 as plots of lift coefficient per unit angle of attack shown as a function of free-stream Mach number. Experimental data are presented here for the same three angles of attack considered in figure 5. In the calculation of the experimental points, the small amount of lift sometimes evident at $\alpha = 0$ (cf. fig. 7) has been ignored as due probably to inaccuracies in the setting of the zero angle (see section "PRECISION OF DATA"). The gap in the solid-line curves of figure 8 corresponds to the range which was not covered in the theoretical calculations of reference 2.[8]

The most significant plot here - indeed in the entire report - is that of figure 8(a), which summarizes the lift results for the front half of the profile. The solid-line curve in this plot shows clearly the increase in initial lift-curve slope which transonic theory predicts in the vicinity of shock attachment. Because of the gap in the theoretical values, the details of the curve at its maximum are in some doubt, though the theoretical lift will certainly remain finite throughout. As one would expect in the light of the previous figures, the experimental data for the smallest angle of attack confirm the theoretical curve remarkably well. Obviously, however, the peak in the data diminishes rapidly with increasing angle; at an angle of attack of 4.2° it has disappeared entirely. At Mach numbers sufficiently removed from the attachment value, the agreement between experiment and theory persists over the complete angle range. As has been seen, this entire behavior is in accord with qualitative considerations regarding the limitations of the theory. The inadequacy of the linear theory near the attachment Mach number is apparent.

---

[8]Note added in proof: Theoretical results for this range are now available in a recent paper by Yoshihara (Yoshihara, Hideo: On the Flow over a Wedge in the Upper Transonic Region. WADC Tech. Rep. 53-478, U. S. Air Force, Nov. 1953).

The results for the rear wedge and complete profile (figs. 8(b) and (c)) are complicated by the viscous effects on the rear of the airfoil. For the rear wedge, the measured values of c_{l_r}/α change markedly with angle of attack throughout the Mach number range, the agreement with theory improving as the angle is increased. The data for the complete profile combine the behavior noted for the individual wedges. The results at the smallest angle of attack, in particular, show a local increase similar to that predicted by theory (as for the front wedge) but fall quantitatively far short of the theoretical values (as for the rear wedge). The results of figure 8(c) would, in fact, present a rather confusing picture in the absence of the foregoing analysis.

As at zero angle of attack, the check between theory and experiment on the front wedge implies that the finite span of the test model had little effect on the lift at the midspan station.

Center of lift.- The experimental and theoretical positions of the center of lift are shown in figure 9 for the front and rear wedges as well as for the complete profile. In all cases, the positions are measured aft from the leading edge of the profile.[9] The experimental values for the rear wedge at $\alpha \cong 0.3^\circ$ are too far forward to be included in any reasonably sized plot and have therefore been omitted.

The results of figure 9 have much the same aspect as those already considered in figure 8. For the front wedge, the data at the lowest angle of attack again confirm the theory remarkably well, considering the increased scatter inevitable in the experimental determination of the center of lift. The deterioration of the theory with increasing angle of attack is, however, less apparent here. For the rear wedge and complete profile, the complicating effects of the viscous phenomena are obvious.

Drag due to angle of attack.- The increase in drag with increase in angle of attack is shown in figure 10 for all of the test Mach numbers. The data are shown here as a function of angle of attack instead of the more usual lift coefficient. This is done so that results for the front wedge and complete profile can be more easily included in the same plot. The theoretical curves have been calculated from the equation

$$c_d - (c_d)_o = \left(\frac{dc_l}{d\alpha}\right)_o \alpha^2 \qquad (3)$$

on the basis of the theoretical values of lift-curve slope given in figure 8. This well-known equation is based on the assumption that the drag due to angle of attack arises solely from the streamwise component of the pressure difference acting between the top and bottom surfaces of the

[9]For the reason already mentioned in footnote 7, the center of lift corresponding to $\xi_\infty = 1.058$ in figure 7 of reference 2 should be at 0.248 instead of at the position originally shown. This change has been incorporated in the present work.

inclined profile. It is valid for a vanishingly thin airfoil at a vanishingly small angle of attack and neglects any leading-edge thrust which might properly be included in the small-disturbance theory when the bow wave is detached. (Whether or not a leading-edge thrust should be included to make up for the erroneous pressure distribution given by the small-disturbance theory in the vicinity of the leading edge is at present an open question. The problem is similar in principle to those discussed by R. T. Jones in reference 36, but the details are more involved in the present case.)

Contrary to the situation with regard to the lift (fig. 7), the theoretical and experimental results of figure 10 show good agreement at the smaller angles of attack ($\alpha<1-1/4^\circ$) only for free-stream Mach numbers above the attachment value. For Mach numbers below this value, the experimental data fall well below the theoretical curves even at small angles. Since this behavior is evident on both the front wedge and complete profile, its cause must apparently be sought on the forward half of the airfoil. This is borne out by the pressure distributions examined earlier in figure 6(a). As has been noted, this figure shows that the individual pressures on the two surfaces of the front wedge are not in as good agreement with theory as is the lift distribution. In particular, at $\alpha = \pm 1.2^\circ$ the general level of pressure on the front wedge is somewhat less positive than the theory would predict near both the leading edge and the ridge line. This reduced pressure acting on the finite thickness of the real airfoil apparently serves to decrease the drag below that calculated on the assumption of a vanishingly thin profile. The phenomenon is even more evident in the pressure data at $\alpha = \pm 4.2^\circ$ (though this may be stretching the theory beyond its justifiable limits). As a result of this effect, the drag at Mach numbers below the attachment value (fig. 10) does not rise appreciably for angles of attack less than 2° and remains comparatively low even at the higher angles. This situation does not prevail at Mach numbers above attachment. The comparison between theory and experiment at Mach numbers below attachment might be improved by the inclusion of a theoretical leading-edge thrust (if such indeed is required). The resulting theoretical curve, however, would still be parabolic and hence not likely to agree in all respects with the experimental data. It would appear that some detailed study of the flow in the vicinity of the leading edge is desirable.

Lift-drag ratio.- The variation with Mach number of the maximum lift-drag ratio (skin friction neglected) for the complete profile is shown in figure 11. The experimental values shown here have been deduced from the results given in figures 4, 7, and 10.[10] The theoretical values have been

[10]No experimental value is shown for $M_\infty = 1.166$, since the data did not extend to a high enough angle of attack at this Mach number.

calculated from the following equation applicable to a parabolic drag curve:

$$\left(\frac{L}{D}\right)_{max} = \frac{1}{2}\sqrt{\frac{(dc_l/d\alpha)_o}{(c_d)_o}} \tag{4}$$

This equation is subject to the same limitations as is equation (3).

At and just above shock attachment, the experimental values of $(L/D)_{max}$ fall appreciably below the curve given by the transonic theory. This is a result primarily of the decrease in lift-curve slope with angle of attack as noted in figure 7. Below shock attachment, the experimental points fall above the theoretical curve. This is traceable to the variation of drag with angle of attack as discussed in connection with figure 10. As a result of the foregoing behavior, the experimental data do not exhibit the maximum which theory shows in the vicinity of the attachment Mach number. The experimental values are, in fact, nearly constant over the entire Mach number range. Obviously, the results of the transonic theory are not valid to a sufficiently high angle of attack to allow the accurate prediction of the maximum lift-drag ratio. The linear theory appears superior here, though in view of the earlier results this must be regarded as purely a matter of luck.

Comparison with Subsonic Results

It is instructive to compare the present lift results with those obtained by Willmarth on a double-wedge airfoil at subsonic speeds (ref. 27). This is done in figure 12, where the present results for $\alpha \cong 1.2^\circ$ are shown together with comparable data for one of the airfoils tested by Willmarth.[11] The data are plotted here in terms of the transonic similarity variables, since the thickness ratio of the airfoils was different in the two tests. Willmarth's data are represented in the same manner as in his report - that is, by vertical lines indicative of the experimental spread.

The most striking thing about figure 12 is the symmetry of the experimental lift data about the vertical axis - that is, about $M_\infty = 1$ (see fig. 12(a)). As has been seen, the peak in the data at supersonic speeds is predictable on the basis of inviscid theory and can be traced to the pressures on the front half of the airfoil. The peak at subsonic speeds, though not yet calculated theoretically, is explained by Willmarth as also due to inviscid causes. Here, however, the effect is associated with the growth of the supersonic region on the rear half of the section. Thus, although there does exist a kind of symmetry in the peaks some distance to

[11] Willmarth's results were linear for $0^\circ < \alpha < 2^\circ$. The Reynolds number of his data is the same as that of the present tests.

each side of $M_\infty = 1$, the causes of this symmetry are themselves not at all symmetrical. This is in contrast to the situation very close to $M_\infty = 1$, where the flow fields adjacent to the airfoil are known to be essentially the same for equal increments above and below the sonic flight speed (see refs. 15 and 37).

The movement of the center of lift with free-stream Mach number does not exhibit the symmetry shown by the lift itself. The results of figure 12(b) have, in fact, a rather antisymmetric appearance with respect to the vertical axis.

General Remarks

Before concluding, it should be emphasized that, in those cases where experiment and the transonic theory agree well, the excellence of the agreement is due, in part, to the use of $(\gamma + 1)M_\infty^2$ in the similarity variables in place of the more usual $(\gamma + 1)$. If only $(\gamma + 1)$ had been used, the agreement would still be qualitatively good but quantitatively much less gratifying. For airfoils thicker than the present one, the agreement between experiment and the small-disturbance theory would, of course, become progressively less satisfactory. For thinner airfoils, the agreement would be expected to improve at first. A condition would eventually be reached, however, at which the boundary layer would be so thick relative to the profile that no inviscid theory would provide a good approximation.

It may also be worthwhile to point out that by accurately predicting the increase in lift-curve slope near shock attachment, the transonic theory has brought to light a result which had not previously been revealed by experiment. The present study thus adds to the growing evidence (cf. refs. 15 through 19, 22 and 23)that the transonic small-disturbance theory is a useful tool for the understanding of the basic phenomena of transonic flow.

CONCLUSIONS

As a result of the foregoing tests, the following conclusions can be drawn regarding the characteristics of a double-wedge profile at Mach numbers near that corresponding to shock attachment at zero angle of attack:

1. As predicted by the transonic small-disturbance theory, the experimental results show a large increase in the initial lift-curve slope at Mach numbers in the vicinity of shock attachment.

2. On the front wedge, where viscous effects are small, the numerical agreement between experiment and theory is generally good at angles of attack up to about $1\text{-}1/4^\circ$. This is true for both the lift distribution and the over-all lift.

3. The foregoing agreement between experiment and theory appears, in general, to deteriorate with increasing angle of attack. As might be expected from qualitative arguments regarding the limitations of the theory, this deterioration proceeds more rapidly the closer the Mach number is to the attachment value. As a result of this behavior, the increase in lift-curve slope near shock attachment disappears at the higher angles of attack.

4. The flow over the rear wedge is critically influenced by shock-wave boundary-layer interaction near the trailing edge. At the smallest angle of attack ($\alpha \cong 0.3^{\circ}$), an unpredicted negative lift is, in fact, observed over the rear 25 percent of the chord. (Such viscous effects would presumably be reduced at Reynolds numbers higher than the value of 0.54 million used in the present tests.)

5. At Mach numbers below shock attachment, the pressure drag increases less rapidly with angle of attack than is predicted by consideration of the theoretical pressure differences between the top and bottom of the airfoil. This is due to the fact that the actual pressures on both surfaces of the front wedge are less positive than the theory predicts. At Mach numbers above shock attachment, the drag due to angle of attack agrees well at small angles with the values given by the theoretical calculations.

6. The measured pressure distribution and drag at zero angle of attack show good agreement with the existing theoretical and experimental results.

7. In support of recent findings by other investigators, the agreement between experiment and transonic theory is found to be greatly improved by the use of $(\gamma + 1)M_{\infty}^{2}$ in place of $(\gamma + 1)$ in the transonic similarity variables.

Ames Aeronautical Laboratory
National Advisory Committee for Aeronautics
Moffett Field, Calif., May 19, 1954

REFERENCES

1. Guderley, Gottfried, and Yoshihara, Hideo: Two-Dimensional Unsymmetric Flow Patterns at Mach Number 1. Jour. Aero. Sci., vol. 20, no. 11, Nov. 1953, pp. 757-768.

2. Vincenti, Walter G., and Wagoner, Cleo. B.: Theoretical Study of the Transonic Lift of a Double-Wedge Profile with Detached Bow Wave. NACA TN 2832, 1952.

3. Guderley, G., and Yoshihara, H.: The Flow Over a Wedge Profile at Mach Number 1. Jour. Aero. Sci., vol. 17, no. 11, Nov. 1950, pp. 723-735.

4. Cole, Julian D.: Drag of a Finite Wedge at High Subsonic Speeds. Jour. Math. and Phys., vol. XXX, no. 2, July 1951, pp. 79-93.

5. Trilling, Leon: Transonic Flow Past a Wedge at Zero Angle of Attack. Zeit. für angewandte Mathematik und Physik, vol. IV, Fasc. 5, Sept. 1953, pp. 358-375.

6. Trilling, L., and Walker, K., Jr.: On the Transonic Flow Past a Finite Wedge. Jour. Math. and Phys., vol. XXXII, no. 1, Apr. 1953, pp. 72-79.

7. Vincenti, Walter G., and Wagoner, Cleo B.: Transonic Flow Past a Wedge Profile with Detached Bow Wave. NACA Rep. 1095, 1952. (Supersedes NACA TN's 2339 and 2588.)

8. Guderley, K. G.: Review 193. App. Mech. Rev., vol. 7, no. 1, Jan. 1954, p. 27.

9. Hilton, W. F., and Pruden, F. W.: Subsonic and Supersonic High Speed Tunnel Tests of a Faired Double Wedge Aerofoil. R.&M. 2057, British A.R.C., 1943.

10. Bartlett, G. E., and Peterson, J. W.: Wind Tunnel Investigation of Double-Wedge Airfoil at Subsonic Speeds. Bumblebee Rep. No. 53, Cornell Aero. Lab., Feb. 1947.

11. Lindsey, W. F., Daley, Bernard N., and Humphreys, Milton D.: The Flow and Force Characteristics of Supersonic Airfoils at High Subsonic Speeds. NACA TN 1211, 1947.

12. Eggers, A. J., Jr.: Aerodynamic Characteristics at Subcritical and Supercritical Mach Numbers of Two Airfoil Sections Having Sharp Leading Edges and Extreme Rearward Positions of Maximum Thickness. NACA RM A7C10, 1947.

13. Pack, D. C.: Investigation of the Flow Past Finite Wedges of 20 deg. and 40 deg. Apex Angle at Subsonic and Supersonic Speeds, Using a Mach-Zehnder Interferometer. R.&M. 2321, British A.R.C., 1946.

14. Pindzola, Michael: Supersonic Tests of Conventional Control Surfaces on a Double-Wedge Airfoil. Jour. Aero. Sci., vol. 17, no. 4, Apr. 1950, pp. 204-210.

15. Liepmann, H. W., and Bryson, A. E., Jr.: Transonic Flow Past Wedge Sections. Jour. Aero. Sci., vol. 17, no. 12, Dec. 1950, pp. 745-755.

16. Stack, John: Experimental Methods for Transonic Research. Proc. Third Anglo-American Aero. Conf., Brighton, Sept. 4-7, 1951, pp. 586-589.

17. Bryson, Arthur Earl, Jr.: An Experimental Investigation of Transonic Flow Past Two-Dimensional Wedge and Circular-Arc Sections Using a Mach-Zehnder Interferometer. NACA Rep. 1094, 1952. (Supersedes NACA TN 2560.)

18. Barish, David T.: Interim Report on a Study of Mach One Wind Tunnels. WADC Tech. Rep. 52-88, U. S. Air Force, Apr. 1952.

19. Griffith, Wayland: Shock-Tube Studies of Transonic Flow Over Wedge Profiles. Jour. Aero. Sci., vol. 19, no. 4, Apr. 1952, pp. 249-257.

20. Laitone, E. V.: A Study of Transonic Gas Dynamics by the Hydraulic Analogy. Jour. Aero. Sci., vol. 19, no. 4, Apr. 1952, pp. 265-272.

21. Hilton, John H., Jr.: Flow Characteristics Over a Lifting Wedge of Finite Aspect Ratio with Attached and Detached Shock Waves at a Mach Number of 1.40. NACA TN 2712, 1952.

22. Sirieix, Maurice, Golaz, Paul, and Rebuffet, Pierre: Résultats expérimentaux obtenus au voisinage de la vitesse du son sur une maquette d'aile à profile losangique. Comptes Rendus de l'Acad. des Sci., tome 235, no. 7, 18 Août 1952, pp. 459-461.

23. Wood, George P.: Experiments on Transonic Flow Around Wedges. NACA TN 2829, 1952.

24. Crossley, Harry E., Jr., and Harleman, Donald R. F.: Studies on the Validity of the Hydraulic Analogy to Supersonic Flow. Part 5. Towed Model Investigations of Transonic Flow. AF Tech. Rep. No. 5985, Pt. 5, U. S. Air Force, Dec. 1952.

25. Donoughe, Patrick L., and Prasse, Ernst I.: Pressure Distributions about Finite Wedges in Bounded and Unbounded Subsonic Streams. NACA TN 2942, 1953.

26. Johnston, G. W.: An Investigation of the Flow about Cones and Wedges at and Beyond the Critical Angle. Jour. Aero. Sci., vol. 20, no. 6, June 1953, pp. 378-382.

27. Willmarth, William W.: The Lift of Thin Airfoils at High-Subsonic Speeds. Ph.D. Thesis, Calif. Inst. of Tech., 1953.

28. Allen, H. Julian: The Asymmetric Adjustable Supersonic Nozzle for Wind-Tunnel Application. NACA TN 2919, 1953.

29. Syvertson, Clarence A., and Savin, Raymond C.: The Design of Variable Mach Number Asymmetric Supersonic Nozzles by Two Procedures Employing Inclined and Curved Sonic Lines. NACA TN 2922, 1953.

30. Busemann, Adolf: Application of Transonic Similarity. NACA TN 2687, 1952.

31. Spreiter, John R., and Alksne, Alberta: Theoretical Prediction of Pressure Distributions on Nonlifting Airfoils at High Subsonic Speeds. NACA TN 3096, 1954.

32. Liepmann, Hans Wolfgang, and Puckett, Allen E.: Introduction to Aerodynamics of a Compressible Fluid. John Wiley and Sons, Inc., 1947, pp. 143-154.

33. Ivey, H. Reese, Stickle, George W., and Schuettler, Alberta: Charts for Determining the Characteristics of Sharp-Nose Airfoils in Two-Dimensional Flow at Supersonic Speeds. NACA TN 1143, 1947.

34. Ferri, Antonio: Experimental Results with Airfoils Tested in the High-Speed Tunnel at Guidonia. NACA TM 946, 1940.

35. Jones, Robert T., and Ames, Milton B., Jr.: Wind-Tunnel Investigation of Control-Surface Characteristics. V - The Use of a Beveled Trailing Edge to Reduce the Hinge Moment of a Control Surface. NACA WR L464, March 1942. (Formerly ARR March 1942)

36. Jones, Robert T.: Leading-Edge Singularities in Thin-Airfoil Theory. Jour. Aero. Sci., vol. 17, no. 5, May 1950, pp. 307-310.

37. Guderley, Gottfried: Two-Dimensional Flow Patterns with a Free-Stream Mach Number Close to One. AF Tech. Rep. No. 6343, U. S. Air Force, May 1951.

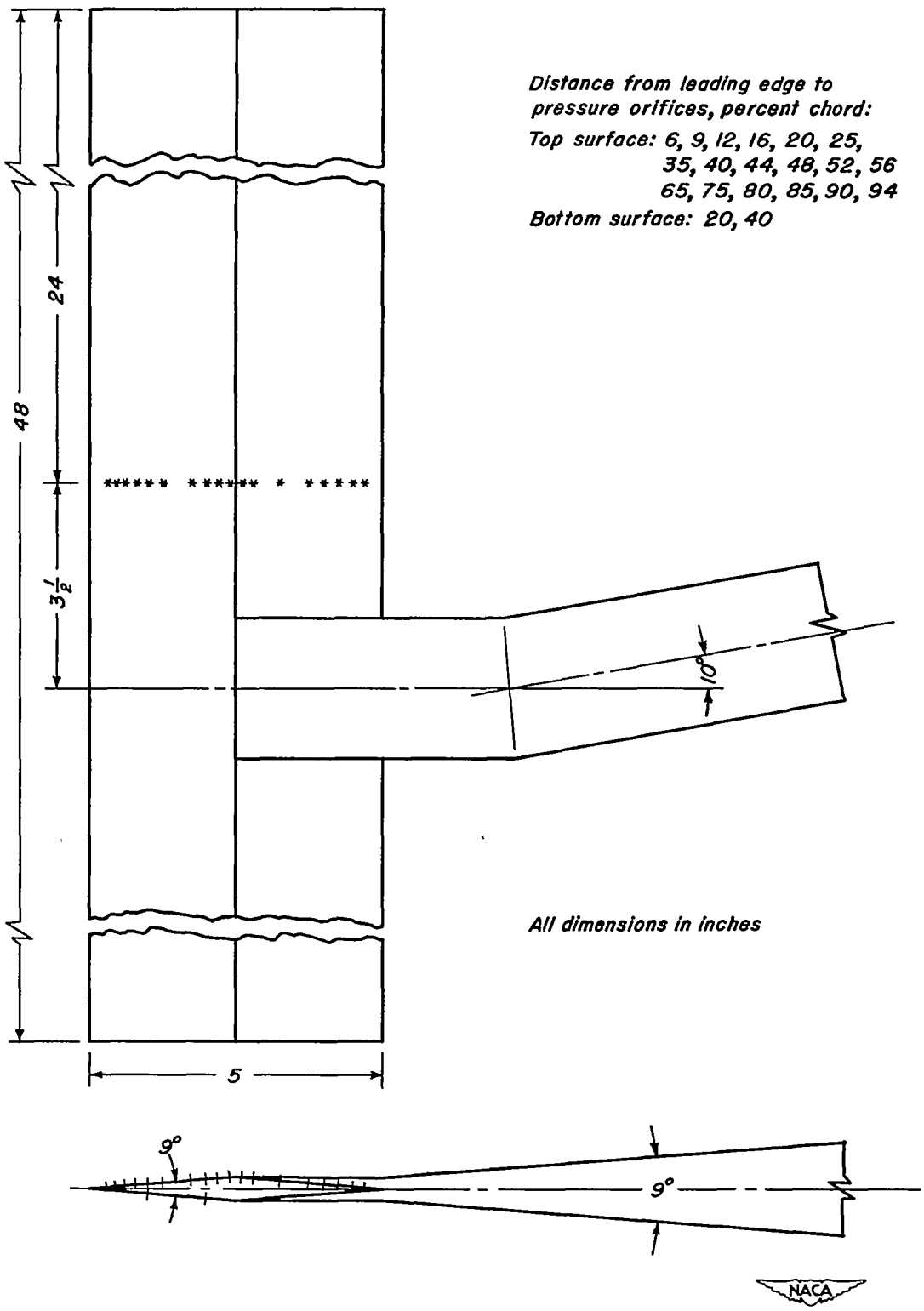

Figure 1.–Drawing of model.

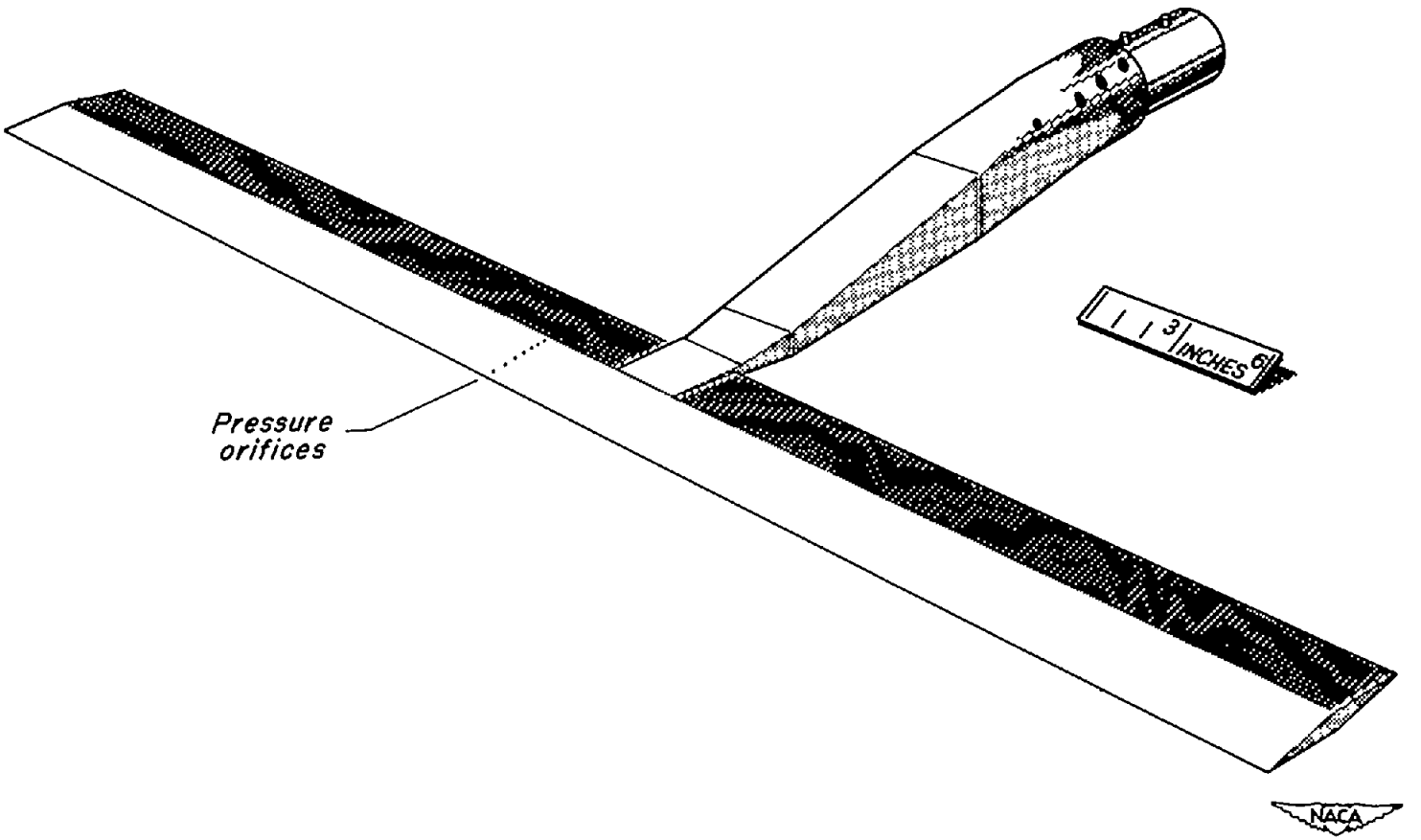

Figure 2.—Sketch of model.

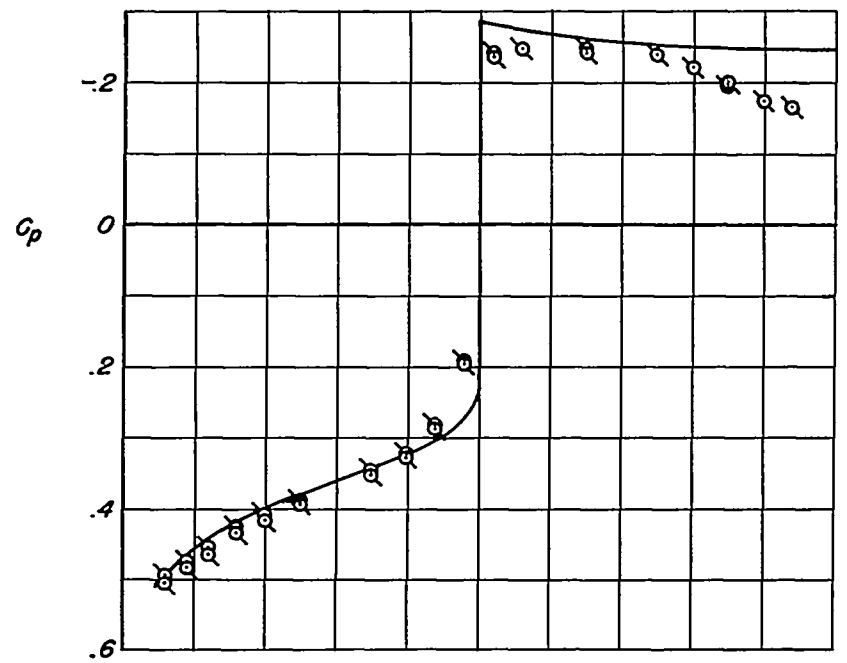

(a) $M_\infty = 1.175$

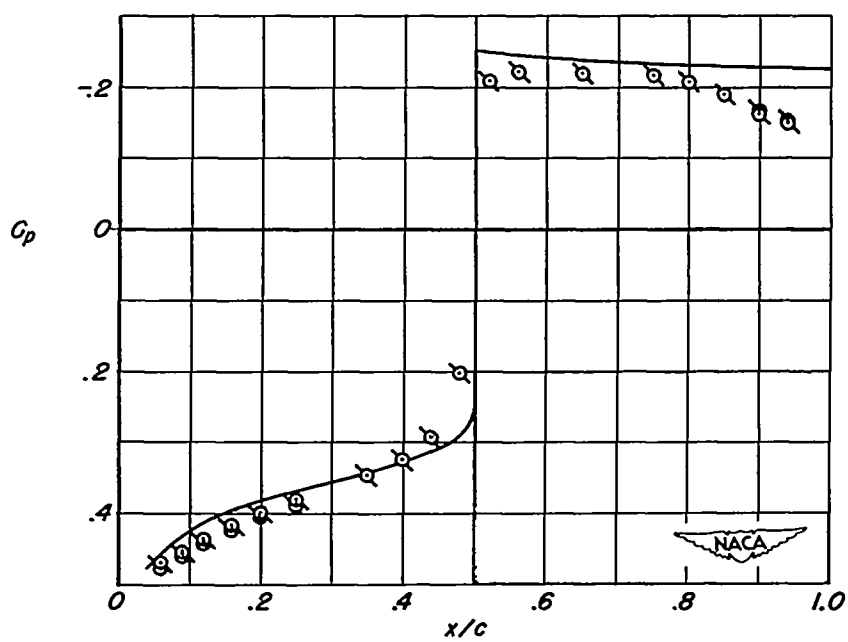

(b) $M_\infty = 1.201$

Figure 3.– Chordwise distribution of pressure coeffcient at $\alpha = 0°$ for four representative Mach numbers.

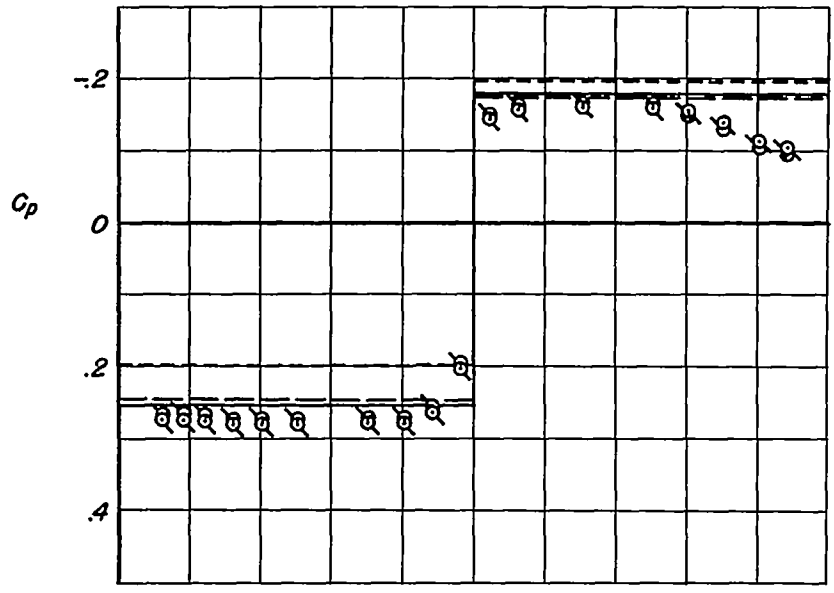

(c) $M_\infty = 1.280$

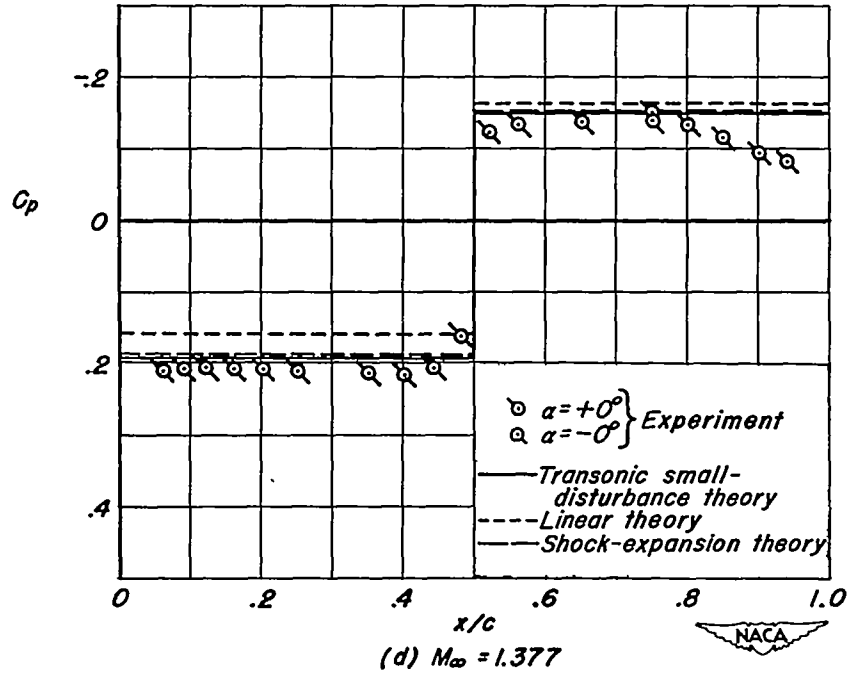

(d) $M_\infty = 1.377$

Figure 3.- Concluded.

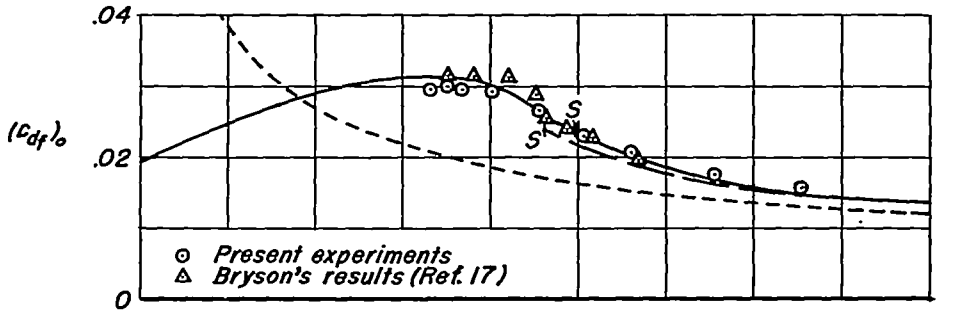

(a) Front wedge.

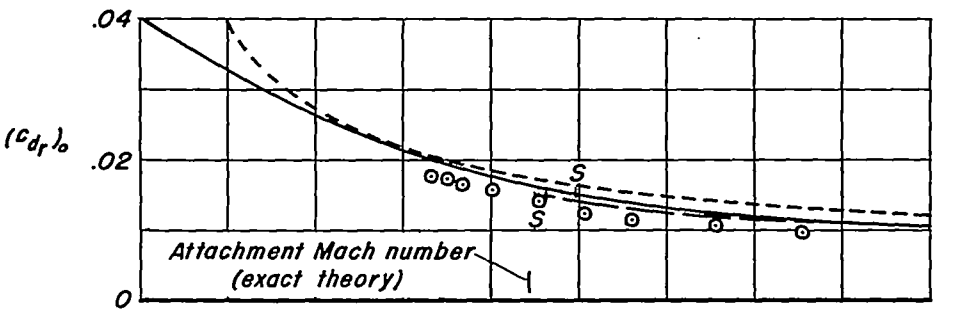

(b) Rear wedge.

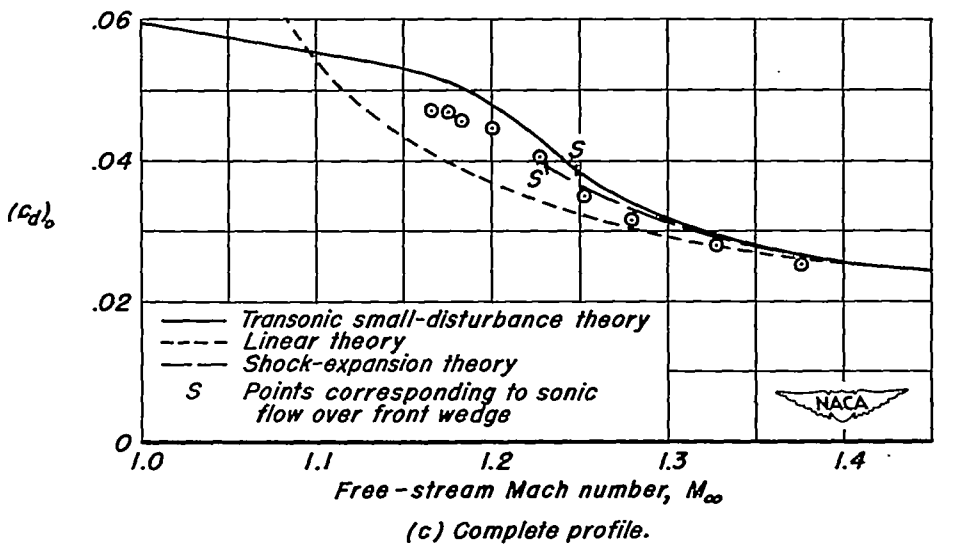

(c) Complete profile.

Figure 4.- Variation with Mach number of pressure-drag coefficient at zero angle of attack.

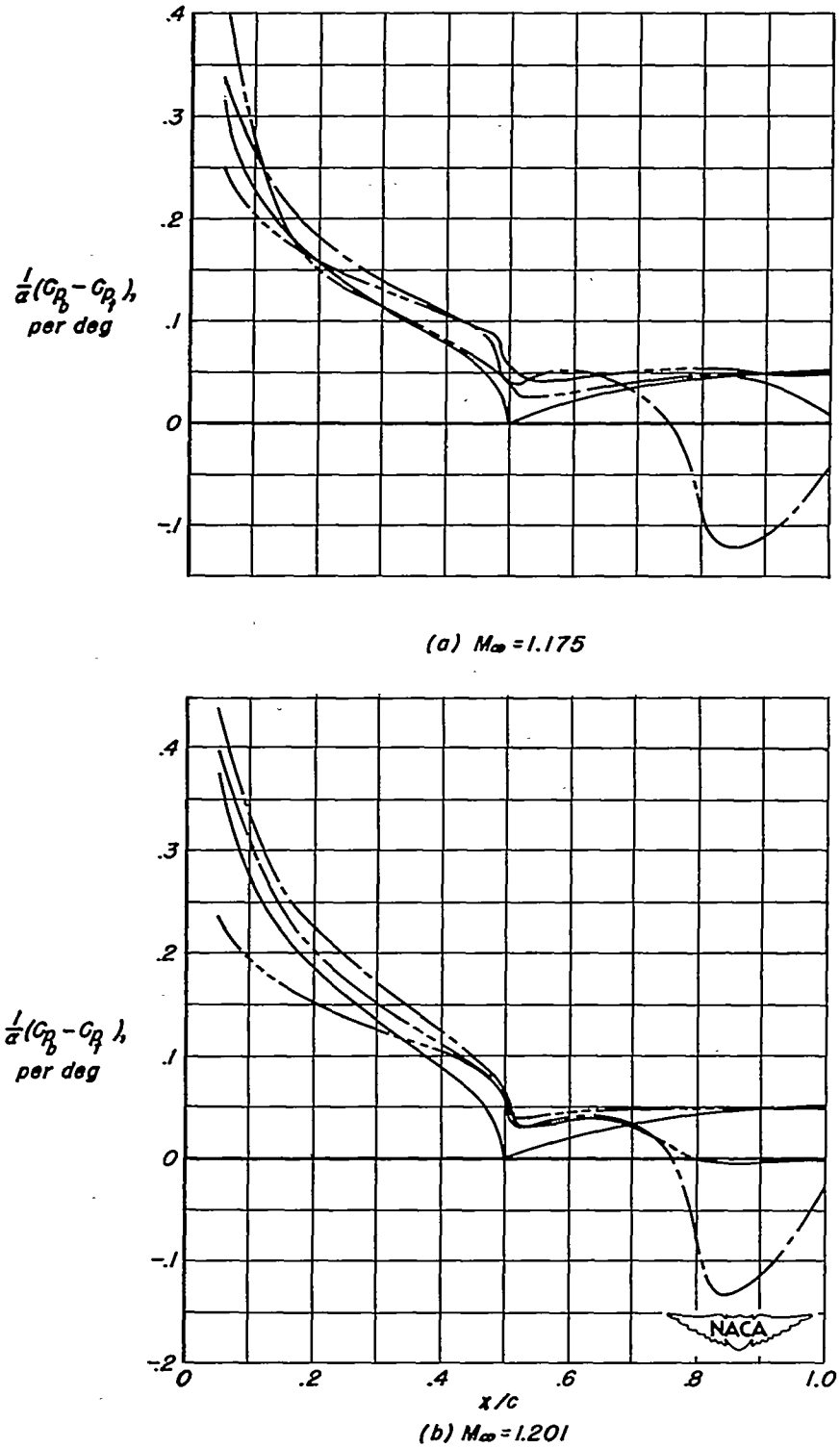

Figure 5.- Chordwise load distribution for four representative Mach numbers.

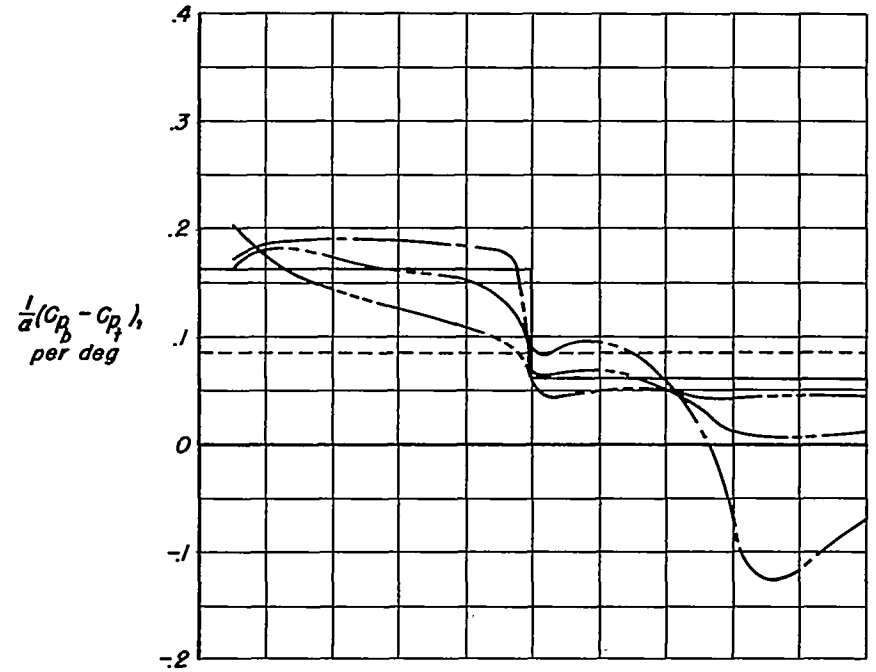

(c) $M_\infty = 1.280$

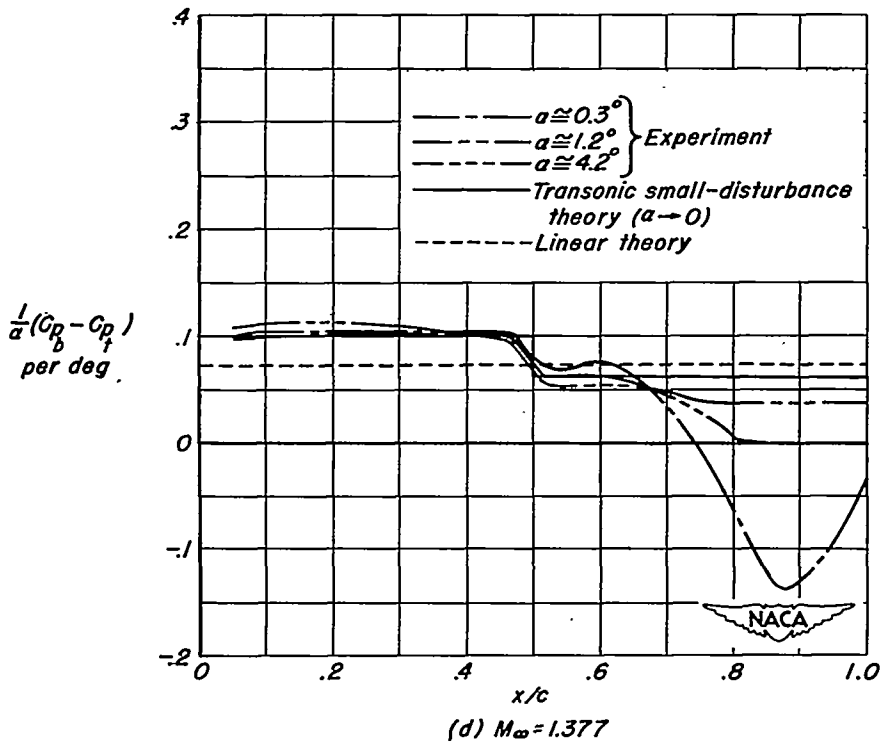

(d) $M_\infty = 1.377$

Figure 5.- Concluded.

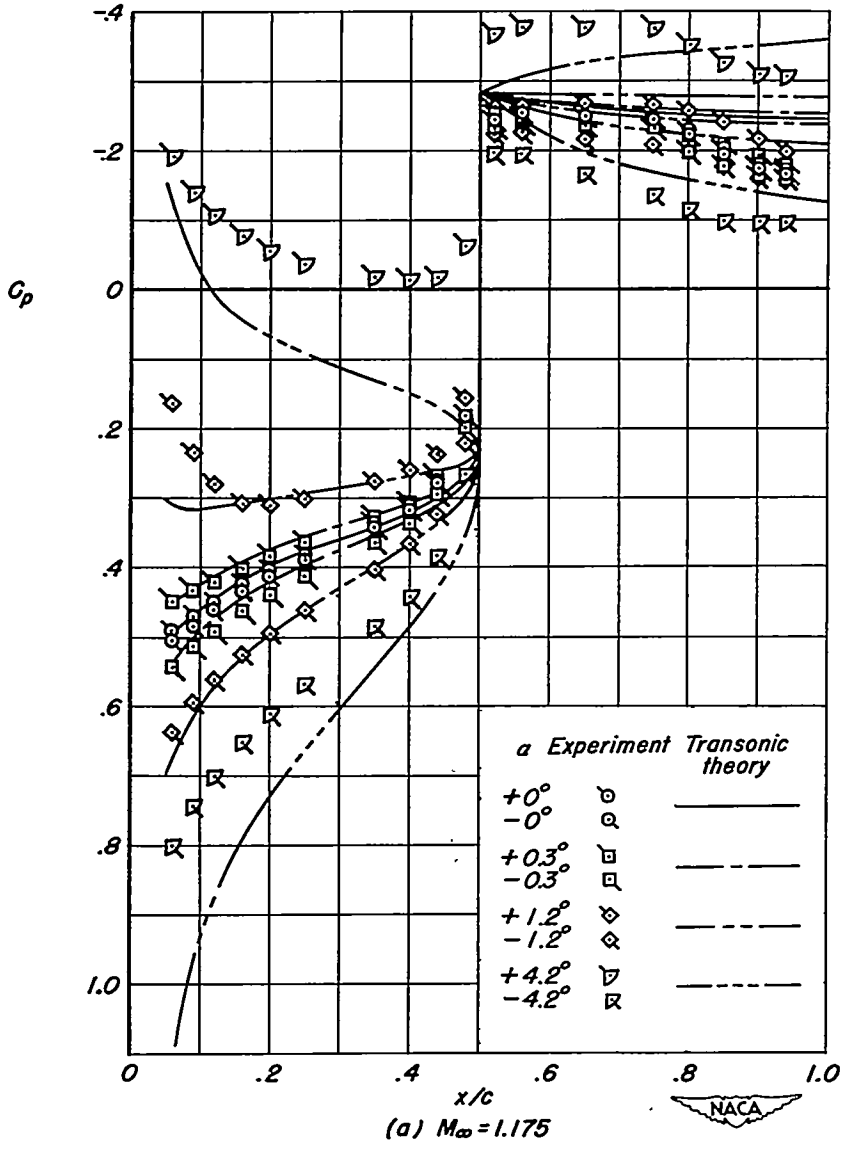

Figure 6.– Chordwise pressure distribution at various angles of attack for two representative Mach numbers.

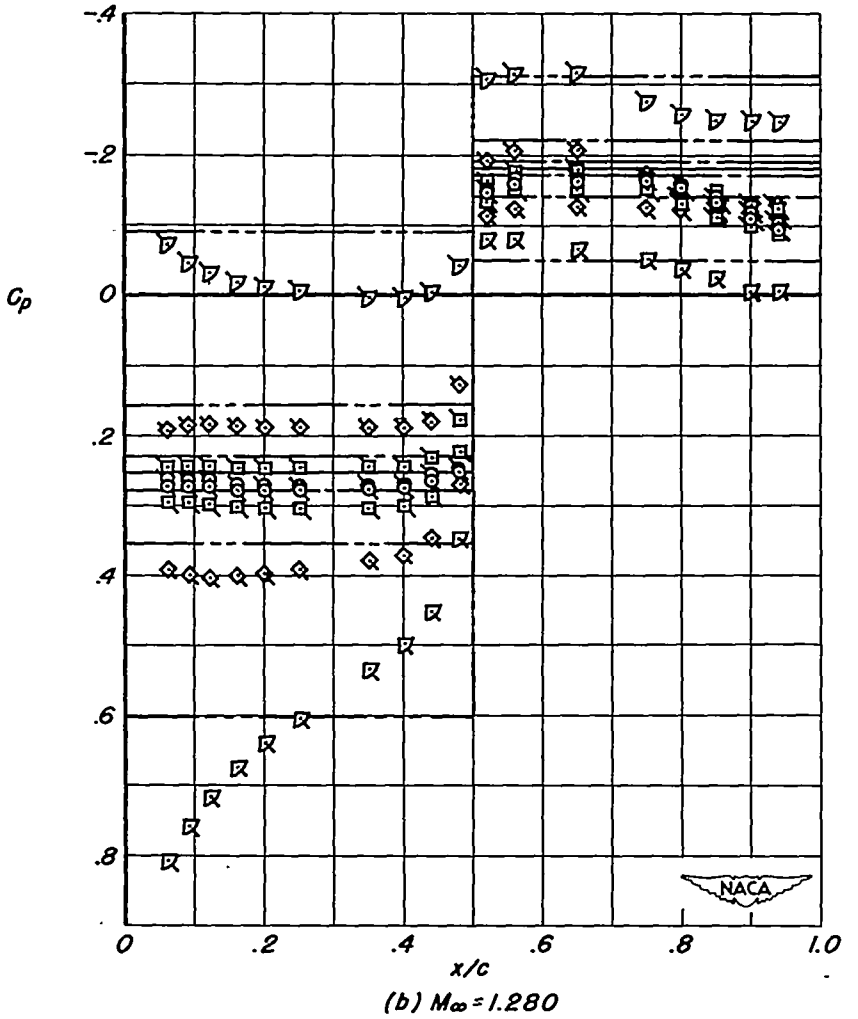

(b) $M_\infty = 1.280$

Figure 6.- Concluded.

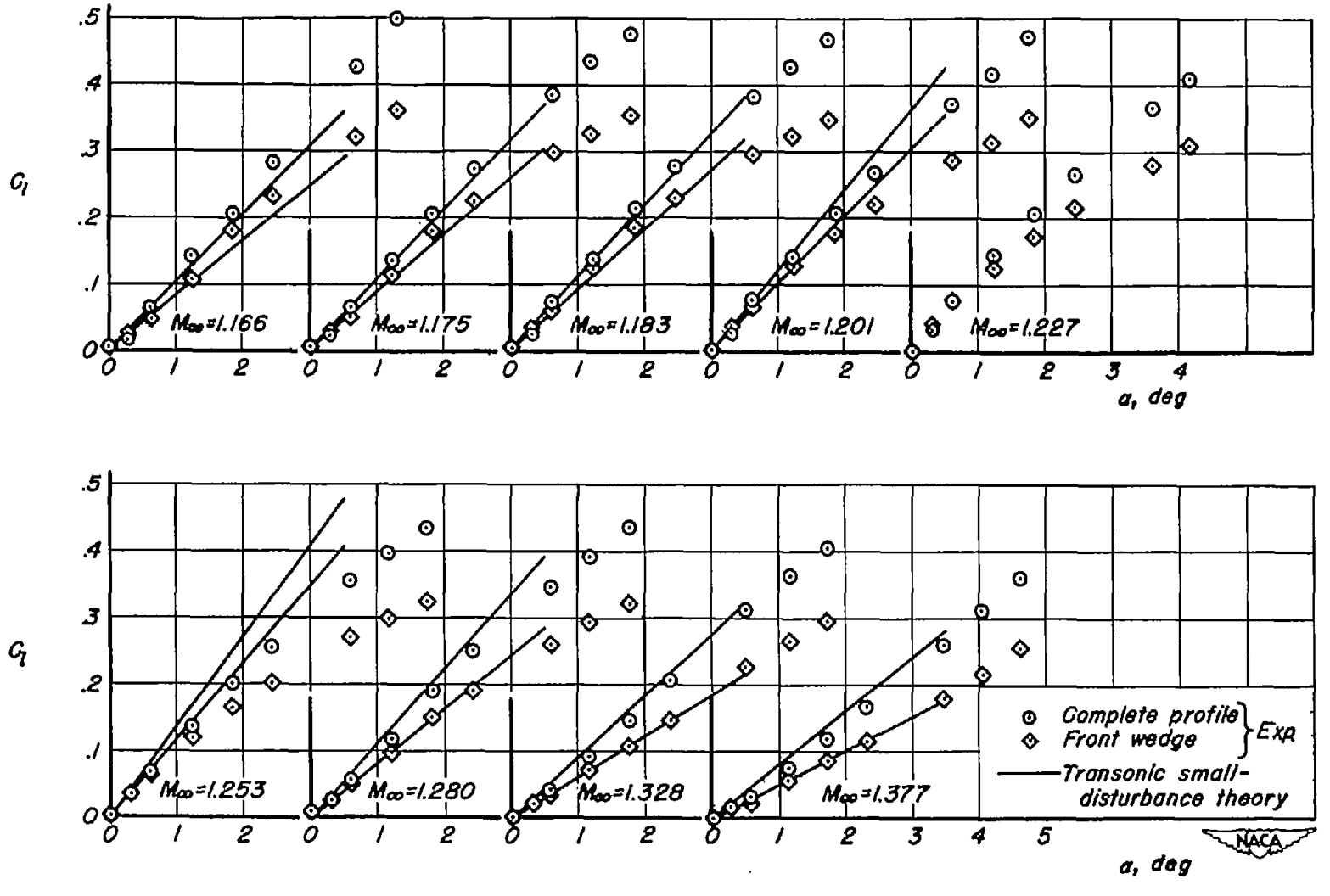

Figure 7.– Lift coefficient as a function of angle of attack for all test Mach numbers.

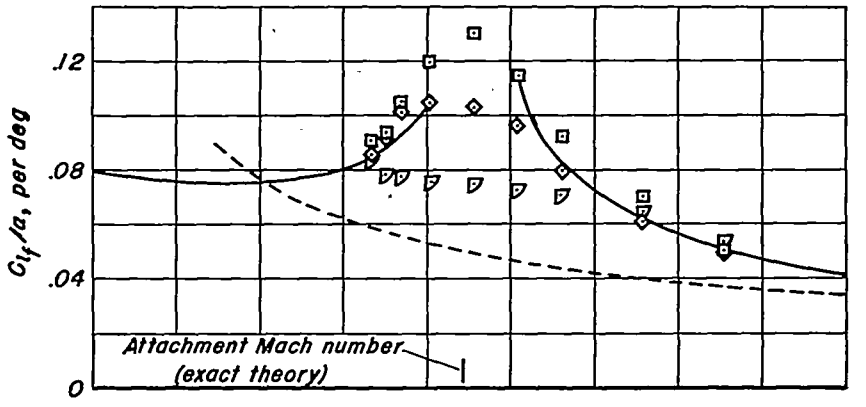

(a) Front wedge.

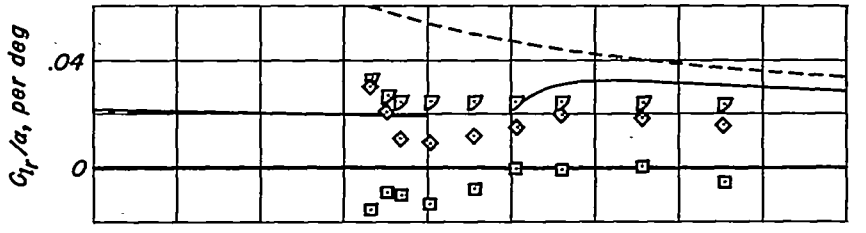

(b) Rear wedge.

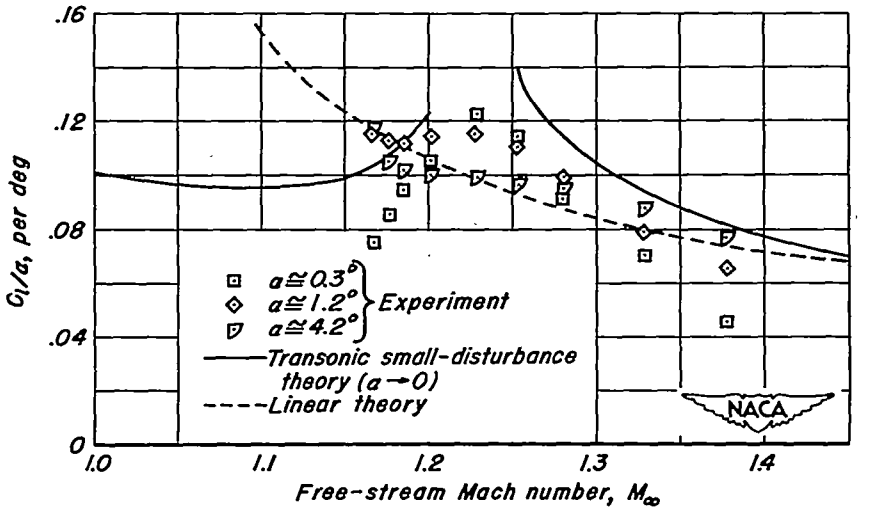

(c) Complete profile.

Figure 8.—Variation with Mach number of lift coefficient per unit angle of attack.

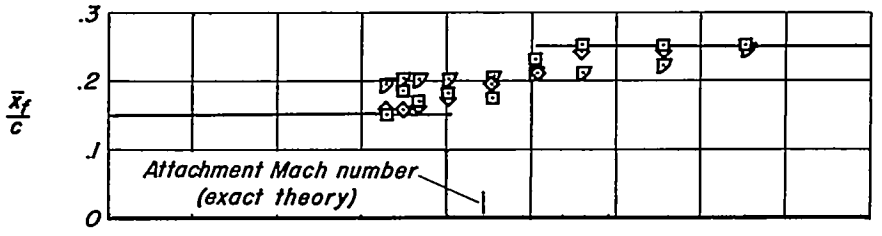

(a) Front wedge.

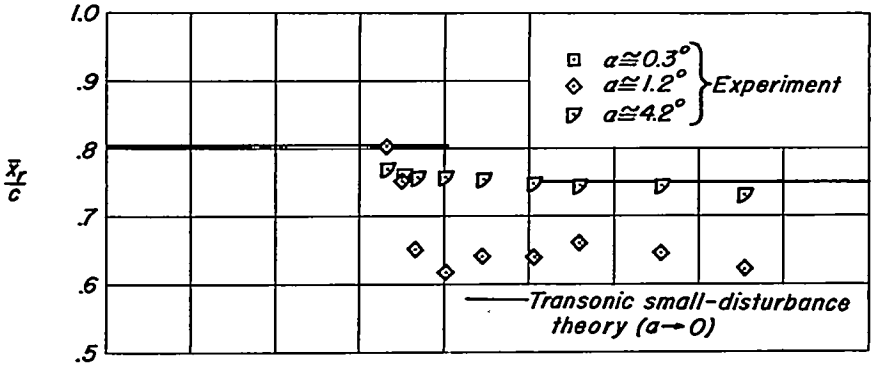

(b) Rear wedge.

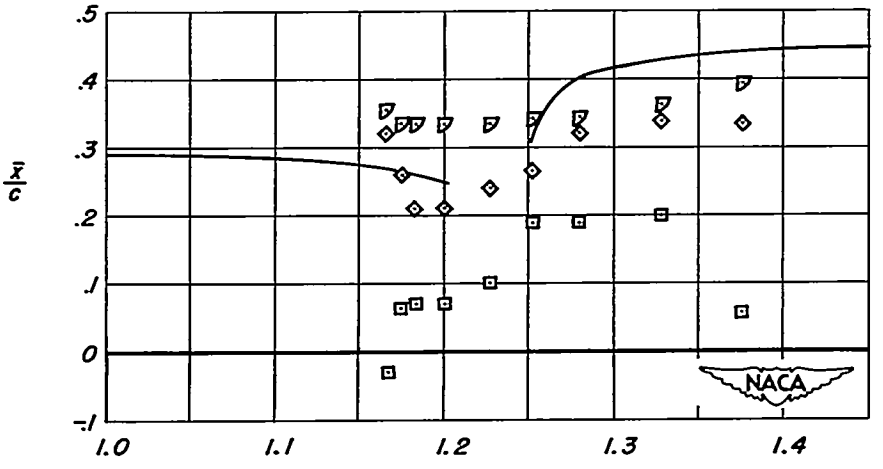

(c) Complete profile.

Figure 9.- Variation with Mach number of chordwise position of center of lift.

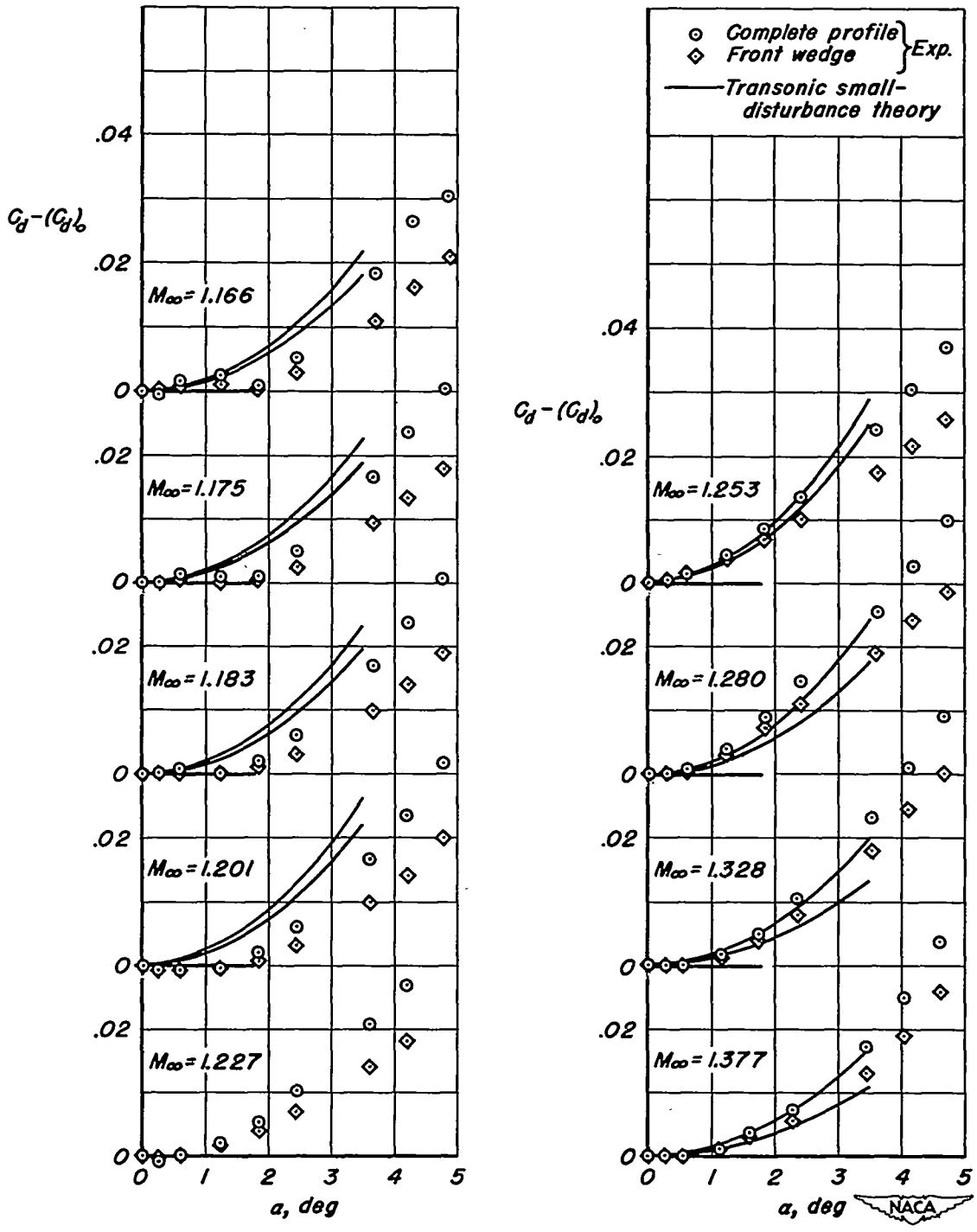

Figure 10.– Increase in pressure–drag coefficient with angle of attack for all test Mach numbers.

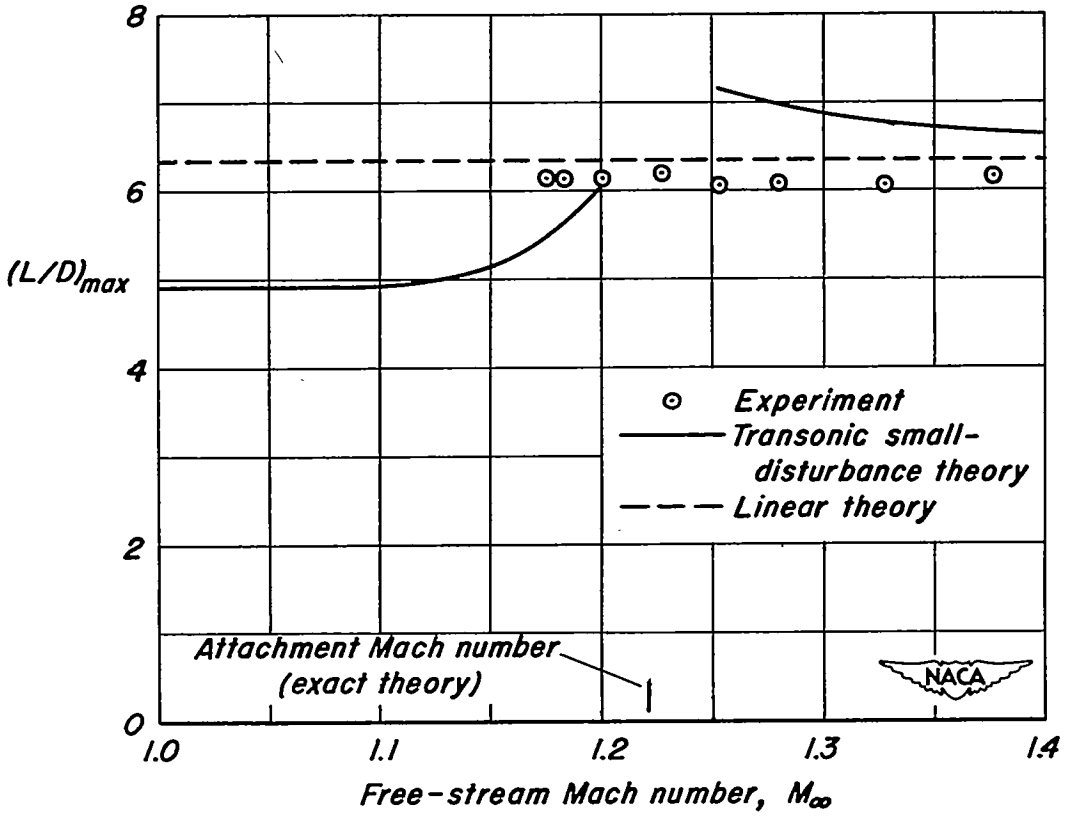

Figure 11.- Variation with Mach number of maximum lift-drag ratio.

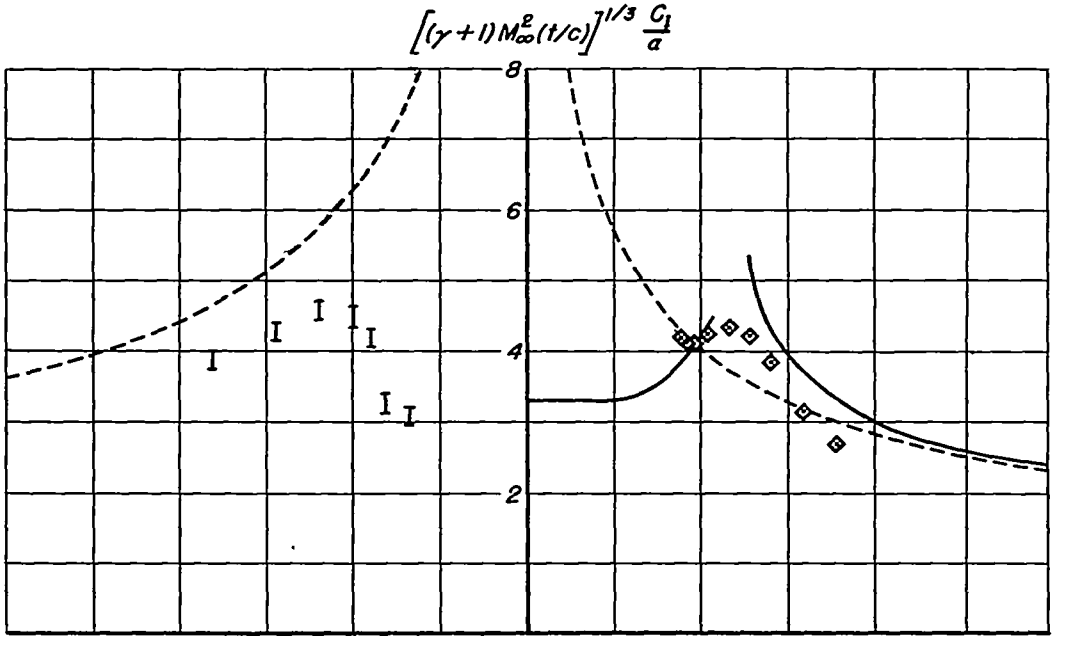

(a) Lift per unit angle of attack.

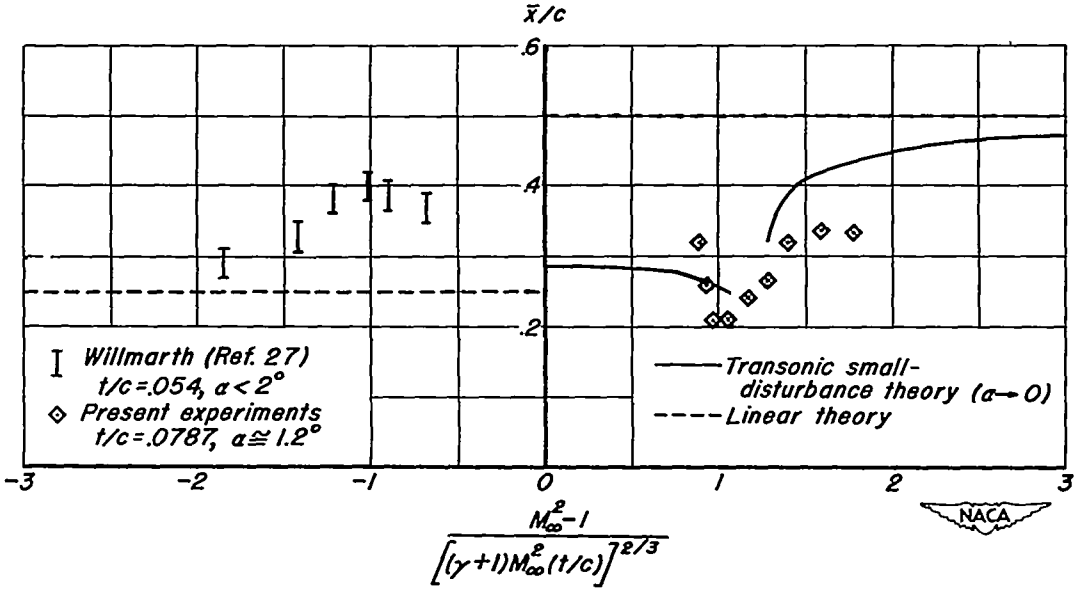

(b) Position of center of lift.

Figure 12.- Lift results in transonic similarity form.

NACA-Langley - 7-22-54 - 1000